



**University of
Zurich**^{UZH}

**Zurich Open Repository and
Archive**

University of Zurich
University Library
Strickhofstrasse 39
CH-8057 Zurich
www.zora.uzh.ch

Year: 2011

Chemotactic antiviral cytokines promote infectious apical entry of human adenovirus into polarized epithelial cells

Lütschg, V ; Boucke, K ; Hemmi, S ; Greber, U F

Abstract: Mucosal epithelia provide strong barriers against pathogens. For instance, the outward facing apical membrane of polarized epithelial cells lacks receptors for agents, such as hepatitis C virus, herpesvirus, reovirus, poliovirus or adenovirus. In addition, macrophages eliminate pathogens from the luminal space. Here we show that human adenovirus type 5 engages an antiviral immune response to enter polarized epithelial cells. Blood-derived macrophages co-cultured apically on polarized epithelial cells facilitate epithelial infection. Infection also occurs in the absence of macrophages, if virus-conditioned macrophage-medium containing the chemotactic cytokine CXCL8 (interleukin-8), or recombinant CXCL8 are present. In polarized cells, CXCL8 activates a Src-family tyrosine kinase via the apical CXCR1 and CXCR2 receptors. This activation process relocates the viral co-receptor $\alpha 3$ integrin to the apical surface, and enables apical binding and infection with adenovirus depending on the primary adenovirus receptor CAR. This paradigm may explain how other mucosal pathogens enter epithelial cells.

DOI: <https://doi.org/10.1038/ncomms1391>

Posted at the Zurich Open Repository and Archive, University of Zurich

ZORA URL: <https://doi.org/10.5167/uzh-48705>

Journal Article

Accepted Version

Originally published at:

Lütschg, V; Boucke, K; Hemmi, S; Greber, U F (2011). Chemotactic antiviral cytokines promote infectious apical entry of human adenovirus into polarized epithelial cells. *Nature Communications*, 2:391.

DOI: <https://doi.org/10.1038/ncomms1391>

Chemotactic anti-viral cytokines promote infectious apical entry of human adenovirus into polarized epithelial cells

Verena Lütschg^{1,2}, Karin Boucke¹, Silvio Hemmi¹ and Urs F. Greber^{1,3}

¹ Institute of Molecular Life Sciences, University of Zurich, Winterthurerstrasse 190, CH-8057 Zurich, Switzerland

² Molecular Life Sciences Graduate School, ETH and University of Zurich

³ corresponding author:

urs.greber@imls.uzh.ch, Telephone: +41 44 635 48 41, Fax: +41 44 635 68 17

Running head: Cytokine-induced apical infection by human adenovirus

Abstract: 148 words

Total text: 3793 words (wo refs, wo meth wo figs legs), max 3500

Refs: 66 (max 70)

Figure: 6 Table: 0

Abstract

Mucosal epithelia provide strong barriers against pathogens. For instance, the outward facing apical membrane of polarized epithelial cells lacks receptors for agents, such as hepatitis C virus, herpesvirus, reovirus, poliovirus or adenovirus. In addition, macrophages eliminate pathogens from the luminal space. We identified a mechanism, in which human adenovirus engages an anti-viral immune response to enter polarized epithelial cells. Blood-derived macrophages co-cultured apically on polarized epithelial cells facilitated epithelial infection. Infection also occurred in the absence of macrophages, if virus-conditioned macrophage-medium containing the chemotactic cytokine CXCL-8 (interleukin-8), or recombinant CXCL-8 were present. In polarized cells, CXCL-8 activated the nonreceptor tyrosine kinase c-Src via the apical CXCR-1 and CXCR-2 receptors. This activation process relocated the viral co-receptor $\alpha\beta 3$ integrin to the apical surface, and enabled apical binding and infection with adenovirus depending on the primary adenovirus receptor CAR. This paradigm may explain how other mucosal pathogens enter epithelial cells.

Introduction

The airway epithelium is both a barrier and early detector for viruses. It involves a cohesive network of polarized cells and restricts the flux of fluids, ions and pathogens into and out of the respiratory organs. An increasing number of pathogenic human viruses are found to be transmitted between mucosal epithelia of individuals, including human immune deficiency virus HIV, influenza virus, enteroviruses, hepatitis A, B, C and E viruses, poxviruses and also human adenoviruses ^{1,2}. Adenoviruses are an environmental risk factor outnumbering the ubiquitous enteroviruses in surface waters ³. Of the 55 human adenovirus types known today (<http://www.vmri.hu/~harrach/AdVtaxlong.htm>), more than one third is associated with disease. Fatal cases of adenovirus infections are mostly due to T-lymphocyte deficiencies and occur in immunosuppressed patients ⁴. In normal individuals, respiratory epithelial cells are initial sites for infection, although the underlying mechanisms are unknown ⁵. This leads to respiratory disease, gastroenteritis, acute hemorrhagic cystitis, meningoencephalitis and conjunctivitis ⁶⁻⁹.

Epithelial cells adhere to each other at cell junctions, which are formed by cadherins, claudins, occludins and nectins and also immunoglobulin superfamily proteins, such as CAR (coxsackievirus adenovirus receptor) and junction adhesion molecule (JAM, ¹⁰). Yet, the junctions are dynamic and allow the passage of immune cells between epithelial cells. This supports inflammatory responses ¹¹, and somehow lays open receptors for viruses like polio, herpes, adeno, coxsackie and reovirus ¹²⁻¹⁴. Since the intact epithelium is resistant to infection, it has remained unknown how viruses cross epithelial barriers.

Some pathogens are known to affect junctional integrity, as for instance enteropathogenic *Escherichia coli*, or the extracellular human gastric bacteria

Helicobacter pylori, which disrupt transepithelial resistance and retarget $\beta 1$ integrin to the apical surface. Activated $\beta 1$ integrin adheres to bacteria and then triggers the injection of effectors into epithelial cells, which induces proinflammatory host genes and the release of cytokines, such as interleukin 8 (CXCL-8) or tumor necrosis factor- α (TNF- α). This in turn attracts and stimulates immune cells to infiltrate mucosa and eventually destroy tissue integrity reviewed in ¹⁵.

Viruses do not appear to drastically affect junctional integrity. Instead, some viruses directly bind to apical receptors. For example, coxsackievirus B, a picornavirus, attaches to CD55, which triggers a signalling cascade leading to virus attachment to the tight junction protein CAR (coxsackie virus B adenovirus receptor) and infectious virus entry ¹⁶. Similarly, the severe acute respiratory syndrome SARS coronavirus adheres to the human angiotensin converting enzyme 2 on the apical membrane of ciliated airway epithelial cells, and infects cells by receptor-mediated endocytosis ^{17,18}. Likewise, sialic acid binding viruses, such as influenza virus, polyomavirus, rotavirus or reovirus attach to the apical side of polarized epithelial cells, although the infectious uptake mechanisms are unknown ¹⁹. Here we provide evidence for a novel mechanism of epithelial infection, namely the stimulation of virus entry by virus-induced cytokines from immune cells.

Results

Macrophages enhance apical Ad5 infection of epithelial cells

CAR localizes to the basolateral domain and tight junctions (TJs) and $\alpha\beta 3/5$ integrins to the basal membrane of polarized airway epithelial cells, which precludes apical

Ad2/5 (adenovirus type 2 and 5) binding and infection ²⁰⁻²². We validated this observation with two different human lung epithelial cell lines, bronchial epithelial 16HBE14o cells and alveolar type II epithelial A549 cells. When grown to confluent monolayers on transwell filters and inoculated with a non-replicating adenovirus reporter, which expresses murine IL-2 (Ad5_mull-2, mull-2 expression is thereafter referred to as infection) ²³, both cell types were poorly infected from the apical side, but were strongly infected from the basolateral side yielding infection levels of 20-40% of nonpolarized cell infections (Fig. 1A). Both cell lines expressed CAR, $\alpha\beta 3$ and $\alpha\beta 5$ integrins (Fig. 1B). Opening up the cell-cell contacts with ethylene-diamine-tetraacetic acid (EDTA) significantly increased apical infection (Fig. 1A), consistent with results from earlier treatments of polarized cells with the divalent cation chelator ethylene-glycol-tetraacetic-acid EGTA, ²¹. These results were confirmed by GFP expression analyses from a replication-defective Ad5-eGFP in 16HBE14o cells (Fig. S1A, B).

We next assessed whether macrophages have an impact on adenovirus infection of epithelial cells. Isolated human peripheral blood mononuclear cells (PBMC)-derived macrophages could not be infected with Ad5_mull-2 up to 45 h post infection (pi), unlike 16HBE14o cells (Fig. S2A). As expected, PBMC-derived macrophages did not express the Ad2/5 attachment receptor CAR, and had moderate levels of $\alpha\beta 3/5$ integrins on their surface (Fig. S2B, ²⁴). To mimic the natural situation of macrophage-controlled mucosal epithelia, we seeded macrophages onto the apical side of polarized 16HBE14o monolayers and allowed attachment for 24 h. Transmission electron microscopy (TEM) of macrophage and HBE co-cultures revealed intact epithelial monolayers with macrophages attached to the apical membranes (Fig. 1C). Upon apical inoculation of co-cultures with Ad5 wildtype for 1 h, virions could be readily detected in vesicular structures of macrophages and to a much lower degree in epithelial cells (Fig. 1C-D). Epithelial cells cultured without macrophages contained no detectable virus particles (not shown). When co-cultures

were inoculated with Ad5_muLL-2 for 20 or 30 h, we detected no significant differences between apical or basolateral inoculations, whereas polarized epithelial cells without macrophages were not infected by apical inoculation (Fig. 1E). These data indicate a crucial role for macrophages in Ad5 infection of epithelial layers consisting of macrophages and epithelial cells.

Apical Ad5 infection does not depend on direct interaction between macrophages and epithelial cells

Macrophage-mediated apical infection either depends on direct interactions of macrophages with epithelial cells, or on messengers secreted from macrophages, such as cytokines. We tested if the supernatant from macrophages inoculated with adenovirus, the so called conditioned medium (CM), was sufficient to increase the Ad5_muLL-2 infection of polarized epithelial cells. PBMC-derived human macrophages were inoculated with Ad2 for 4 h, the medium collected and cleared by centrifugation and added to polarized 16HBE14o cells for 4 h, followed by apical inoculation with Ad5_muLL-2 for 20 or 30 h (Fig. 2A). Stimulation of polarized cells with CM led to strong increase of apical infection compared to non-stimulated cells (Fig. 2B). Although we observed variations of CM potencies between macrophages from different blood donors, the typical increase of viral infection was 8-12 fold. In all instances, the maximal stimulation of apical infection was obtained at 4-8 h post stimulation (Fig. 2C). Interestingly, the infection stimulation was much stronger, if CM was applied apically than basolaterally, and was only marginally increased by simultaneous addition to both apical and the basal domains compared to apical stimulation (Fig. 2D). Importantly, the CM did not lose its potency by previous centrifugation under conditions, which completely pelleted viral particles (Fig. S3A). Heat inactivation of CM at 75°C for 15 min reduced the stimulatory activity to almost background levels suggesting that heat sensitive factor(s) were responsible for the infection stimulating effects (Fig. S3B). Taken together the data suggest that adenovirus inoculated macrophages condition the medium with heat sensitive agents,

which act on the epithelial cells from the apical side and enhance apical adenovirus infection.

CM does not alter epithelial integrity but enhances apical binding of Ad2/5

We measured the transepithelial electrical resistance (TEER) or diffusion rate of 10 kDa dextran-FITC across the epithelial layer. Treatment of polarized 16HBE14o cells with CM or control macrophage supernatant did not indicate any impairment of epithelial integrity, whereas EDTA treatment drastically reduced TEER and increased dextran diffusion (Fig. 2E). In a binding assay, we next analyzed the localization of atto565-labeled Ad2 added to polarized 16HBE14o cells by incubation at 4°C. Side projections of confocal fluorescence microscopy z-stacks revealed an increased apical localization of Ad2-atto565 on CM-treated cells compared to cells treated with control macrophage supernatant (Fig. 2F-G). We did not detect viral particles in basolateral areas, or within cells suggesting that the epithelial layers were intact. We conclude that enhanced apical infection upon CM treatment is not due to disrupted junctions, but rather results from changes in the apical membrane domain composition allowing for virus attachment.

CXCL-8 mediates apical adenovirus infection

Adenoviruses are known to trigger the secretion of cytokines from macrophages, which coordinate a concerted anti-viral immune response²⁵. To identify cytokines in the infection stimulating CM, we performed a BioPlex[®] assay including 12 different cytokines with known effects on epithelial layers. At 4 h after inoculation of macrophages with adenovirus, we detected interleukin (IL)-6, CXCL-8, IL-10 and TNF- α in the supernatant, and at 8 h, also interferon (IFN)- γ but no longer IL-10 (Fig. S4). We did not detect IL-1 β , IL-4, IL-12/p70, IL-13, IL-15, IL-17 or IFN- α 2, suggesting that these cytokines have no decisive role in stimulation of epithelial

infection. The treatment of polarized 16HBE14o cells with recombinant human CXCL-8 (CXCL-8), however, boosted apical infection in a dose-dependent manner, albeit not to the full extent as CM. Recombinant human IFN- γ (IFN- γ) had no infection-supporting impact (Fig. 3A), although it increased the expression of MHC-II epitopes on A549 cells (data not shown). The depletion of CXCL-8 from CM with a neutralizing antibody, however, significantly reduced the stimulation of apical infection, whilst depletion of IL-10 did not (Fig. 3B). These data suggest an important role of CXCL-8 in stimulating apical adenovirus infection, although it did not account for the full stimulation by CM. This conclusion was corroborated by the finding that blocking of the CXCL-8 receptors CXCR-1 and CXCR-2 with neutralizing antibodies prior to stimulation with CM reduced CM-mediated infection to a significant extent, yet not completely (Fig. 3C). Neutralization of both receptors together did not have additive effects, suggesting a co-dependency of receptor function by heterodimerization, as suggested earlier reviewed in ²⁶.

CXCR-1 and CXCR-2 are known to be internalized upon ligand activation ²⁷, which initiates CXCL-8 signalling ²⁸. We found that CM-stimulated polarized epithelial cells efficiently internalized both receptors within 10 min, which is consistent with a high degree of activation (Fig. 3D). Interestingly, both CXCR-1 and CXCR-2 were found on the apical side of polarized 16HBE14o cells by confocal imaging (Fig. 3E), supporting the finding that apical application of CM stimulated infection of 16HBE14o cells (Fig. 2D).

CM and CXCL-8 induce apical localization of $\alpha v \beta 3$ integrin coreceptors

Our earlier results indicated that CM did not affect the integrity of the epithelial layer excluding the possibility that receptors become accessible to apical virus particles by loosened cell-cell contact areas. We next tested if integrin receptors were expressed

on the apical surface of CM-stimulated polarized epithelial cells. Flow cytometry measurements indicated that both CAR and $\alpha\beta 5$ integrin total surface expression levels did not change upon CM stimulation while the expression of $\alpha\beta 3$ integrin was slightly decreased (Fig. 4A).

We examined the localization of $\alpha\beta 3$ and $\alpha\beta 5$ integrins in polarized 16HBE14o cells by confocal fluorescence microscopy. Intriguingly, side projections of z-stacks revealed that $\alpha\beta 3$ integrin was present on the apical membranes upon stimulation by CM or CXCL-8 (Fig. 4B), whereas $\alpha\beta 5$ integrin remained localized to the basolateral domains (Fig. S5A-B). The treatment of CM with neutralizing antibodies against CXCL-8 prior to stimulation abrogated the apical localization of $\alpha\beta 3$ integrin (Fig. 4B, C). We confirmed these results by selective biotinylation of the apical cell surface and subsequent neutravidin pull-downs of biotinylated proteins (Fig. 4D). Further analysis by SDS-PAGE and Western blotting identified $\beta 3$ integrin as one of the biotinylated, thus apical proteins. The membrane cofactor CD46, which was reported to localize to the apical membrane compartment²⁹, was also significantly biotinylated from the apical side, similar to $\beta 3$ integrin (Fig. 4D). We next tested the functional significance of the apical localization of $\alpha\beta 3$ integrin upon CM stimulation. Apical addition of anti- $\alpha\beta 3$ integrin function blocking antibodies to CM-stimulated 16HBE14o cells strongly reduced Ad5_mull-2 infection, while anti- $\alpha\beta 5$ integrin antibodies had no significant effects (Fig. 4E).

We further confirmed the role of the receptors $\alpha\beta 3$ integrin and CAR in apical infection upon CM stimulation with competition experiments. Soluble forms of CAR and integrin receptors added after the 4 h stimulation period were able to interfere with infection in a dose-dependent manner (Fig. 4F). Control soluble CD46, however, had no effect. Likewise, soluble Ad2 fiber knob inhibited infection whereas Ad35 fiber knob, which does not bind CAR, showed no effect (Fig. 4G). In agreement with these

functional interference data, we found CAR epitopes on the apical side of CM stimulated 16HBE14o cells, distinct from the tight junction marker ZO-1 (Fig. S5C).

These results were in line with the colocalization of $\alpha\beta3$ integrin and CAR with Ad2-atto565 particles added apically to stimulated cells (not shown). Together, the data suggest that CM or CXCL-8 enhance the localization of $\alpha\beta3$ integrin and CAR to the apical domain without grossly altering the overall cell surface expression of $\alpha\beta3$ integrin. This enables adenovirus attachment to the apical cell surface and subsequent infection.

$\beta3$ integrin relocation and CM-mediated apical infection are Src-dependent

To address the nature of apical $\alpha\beta3$ integrin-mediated adenovirus infection, we tested the hypothesis that a mechanism akin to emerging focal complexes could be involved, which is also implicated in cell migration and wound healing^{30,31}. Focal contacts around integrins mediate cell adhesion to the extracellular matrix. They are dynamically regulated in migratory cells by tyrosine kinase signalling³². It is of note that the chemokine CXCL-8 not only acts as an important chemo-attractant to neutrophils and initiates directed cell migration, it has also been implicated in inducing wound healing and migration of epithelial and endothelial cells³³. CXCL-8 leads to formation of focal complexes by signalling via Src/FAK and paxillin³⁴. We tested if signalling via Src and paxillin is involved in $\alpha\beta3$ integrin relocation. Serum-starved 16HBE14o cells were stimulated with either control medium (supernatant of non-inoculated macrophages), CM, CXCL-8 or CXCL-8 depleted CM for 10 min or 4 h. Strong induction of Src tyrosine 416 (Y416) phosphorylation could be detected in both CM and CXCL-8-treated cells at 10 min or 4 h post treatment (Fig. 5A). Likewise, phosphorylation of paxillin on the critical tyrosine residue Y118 was induced

by CM and CXCL-8 at 4 h, and confirmed by immunofluorescence microscopy, which showed apical localization of pY118 paxillin (Fig. 5B, Fig. S6A).

To test if Src family tyrosine kinases were involved in CM-mediated apical infection, we blocked Src activity with the small compounds PP1 and PP2 ³⁵. The treatment of polarized 16HBE14o cells with PP1 and PP2 prior to CM stimulation had no effects on TEER (Fig. S6B). However, both compounds blocked CM-mediated infection at 10 μ M concentrations (Fig. 5C). Western blot analysis showed that PP1 and PP2 not only inhibited Src and pY118 paxillin phosphorylation, but also blocked the apical localization of $\alpha\beta$ 3 integrin in CM-stimulated 16HBE14o cells (Fig. 5D-E). The data suggest that Src controls β 3 integrin redistribution and apical adenovirus infection (Fig. 6).

Discussion

Cells of the innate immune system, including macrophages and dendritic cells control the inflammatory response by interacting with epithelial cells. Alveolar macrophages are sensors for infection and detect adenoviruses in the airway lumen ³⁶. Upon contact with viruses, they undergo rapid activation and secrete pro-inflammatory cytokines, such as IL-6, CXCL-8 and TNF- α ^{37,38}. This boosts the anti-viral response, attracts leukocytes to the site of infection and critically contributes to mounting adaptive immune responses against the virus. However, activated macrophages also trigger acute lung injury and thereby exacerbate viral infection ³⁹.

Our study here identifies a mechanism, by which activated macrophages increase viral infection of polarized epithelial cells. We show that macrophages co-cultured with polarized epithelial cells on the luminal side take up virus particles and secrete cytokines, which enhance infection of the epithelial cells with adenovirus. This cytokine response does not impair the barrier function of the epithelial cells and does not require the presence of macrophages, suggesting that the infection route depends on a viral receptor in the apical epithelial membrane rather than direct transmission of viral particles from macrophages to epithelial cells, for example a “Trojan-horse” mechanism as proposed for measles virus ⁴⁰.

Cytokine mRNAs and proteins, including IL-6, CXCL-8 are induced in response to adenovirus infection in several cell lines and also *in vivo* ^{41,42}. For example, CXCL-8 was elevated in bronchial alveolar lavage fluid of macaque monkeys upon inoculation of an adenovirus vector encoding the cystic fibrosis gene, and enhanced tissue toxicity ⁴³, or the proinflammatory cytokines TNF- α , IL-6 and CXCL-8 were strongly induced in children with symptomatic human adenovirus viremia after stem cell transplantation ⁴⁴. In epithelial cells, the genomes of adenoviruses counter the anti-viral effects of the cytokines by expressing early region 3 genes, and thereby downregulate cytokine mRNAs and protein levels ⁴⁵. In macrophages, however, the levels of viral gene expression are low, possibly due to inefficient delivery of viral genomes to the nucleus (reviewed in ³⁶). Hence, we readily found four of twelve tested cytokines in virus conditioned macrophage medium, that is CXCL-8, IL-6, TNF- α and IFN- γ .

While IFN- γ had no effect, recombinant chemokine CXCL-8 and activation of its receptors CXCR-1/2 strongly enhanced the infection, although not to the full extent as CM. CM was more potent than isolated cytokines in stimulating infection of nonpolarized cells but the specific components of CM responsible for these effects are unknown. In contrast, the CXCL-8 ligand-receptor pair is best known for its

angiogenic and neutrophil chemotactic properties ^{46,47}. CXCL-8 driven chemotaxis can be elicited in many cell types expressing CXCR-1/2. It plays an important role in fibroblast-mediated wound healing ⁴⁸, the formation of tumor metastases ⁴⁹, and neutrophil chemotaxis ⁴⁸. Chemotaxis forms and dismantles focal complexes and adhesions and dynamically modulates anchorage of cells to the extracellular matrix. Anchorage involves $\alpha\beta3$ integrin, initially in the leading edge of migrating cells ^{31,50}. Intriguingly, CXCL-8 enhancement of apical adenovirus infection required the induced localization of $\alpha\beta3$ integrin in the apical plasma membrane of the polarized epithelial cells, as indicated by neutralizing antibodies or soluble $\alpha\beta3$ integrin competition, which also blocks infection of nonpolarized cells ⁵¹. $\alpha\beta3$ integrin plays an important role in viral infections, where it serves as an affinity regulated coreceptor by binding to a 50 amino acid RGD stretch of the adenoviral capsid protein penton base ^{52,53}, and also critically contributes to HIV infection of adherent macrophages ⁵⁴.

Chemotaxis critically involves the non-receptor tyrosine kinase family Src and paxillin, a pivotal signalling integrator and scaffolding protein ^{32,55,56}. Src directly binds the cytoplasmic tail of $\beta3$ integrin and is activated by $\alpha\beta3$ integrin ^{57,58}, which might induce a positive feedback loop for integrin and Src activation. Activated Src undergoes autophosphorylation on tyrosine 416 inducing a complex with focal adhesion kinase (FAK), which then phosphorylates paxillin on its critical tyrosine residue 118 ^{55,59-61}. The stimulation of polarized epithelial cells with conditioned medium leads to Src phosphorylation at Y416 and paxillin at Y118, indicating that this pathway is activated. This pathway is crucial for infection, since inhibition of Src family tyrosine kinases with PP1 and PP2 leads to loss of Src and paxillin phosphorylation, failure of $\alpha\beta3$ integrin relocalization, and abrogated the infection stimulation. Paxillin may function in $\alpha\beta3$ trafficking or as a component of a retention mechanism holding $\alpha\beta3$ on the apical membrane upon stimulation. Collectively, the data strongly suggest that the conditioned macrophage medium enhances apical

infection by the formation of focal contacts and adhesion sites that are normally found in migratory cells.

In addition to prominent apical localization of focal contact proteins, macrophage conditioned medium also enhanced the localization of CAR on the apical membrane. CAR has been reported to potentially colocalize with $\alpha\beta$ 3 integrin in lipid-rich membrane patches ^{62,63}. It critically supports infection, as indicated by soluble CAR and viral fiber knob competition experiments. In normal polarized epithelial cells, CAR is restricted to the baso-lateral domain and tight junctions by an intracellular trafficking mechanism involving the clathrin-adaptor AP1B ⁶⁴. Whether CAR is specifically delivered to the apical membrane or released from tight junctions remains to be investigated. In any case, the virus makes CAR available for apical infection. In doing so, it takes advantage of anti-viral functions of CAR on epithelial cells, where CAR binds JAML from neutrophils, and thereby supports the infiltration of immune cells at sites of cell injury and infection ⁶⁵. Strikingly, epithelial CAR also enhances wound-healing in mucosal tissue by activating and binding to JAML on gamma-delta T-cells ⁶⁶. These cells have key roles in primary defense of epithelial barriers against infection, traumatic insults and malignancies. These cells might play pivotal roles in the defense against adenoviral infection, and if impaired contribute to the severe pathological conditions in immunocompromised individuals.

Collectively, our results uncover a novel apical infection route for adenovirus. We showed that innate immune cells release CXCL-8, which triggers a signaling cascade in polarized epithelial cells resembling the induction of cell migration. During this process, Src and paxillin are tyrosine phosphorylated on critical residues. The latter is recruited to the apical membrane together with $\alpha\beta$ 3 integrin, depending on Src. In the course of this activation, the immune modulator CAR is localized to the apical membrane and becomes available for binding of virus, which together with $\alpha\beta$ 3

integrins triggers viral uptake and infection. This infection mechanism allows viral pathogens to take advantage of immunological anti-viral reactions and gain entry into a well protected epithelium. We anticipate that similar strategies are used by other viruses whose receptors are not available for virus binding in an intact uninjured epithelium.

Materials and Methods

See Supplemental Information.

Acknowledgements

We thank Dr. Dieter Gruenert for supplying 16HBE14o cells and Dr's Nina Wolfrum, Stefan Kälin and Maarit Suomalainen for discussions and comments to the manuscript. This work was supported by the Swiss National Science Foundation to UFG.

References

1. Cone, R.A. Barrier properties of mucus. *Adv Drug Deliv Rev* **61**, 75-85 (2009).
2. Jackson, D.J. & Johnston, S.L. The role of viruses in acute exacerbations of asthma. *J Allergy Clin Immunol* **125**, 1178-1187; quiz 1188-1179 (2010).
3. Mena, K.D. & Gerba, C.P. Waterborne adenovirus. *Rev Environ Contam Toxicol* **198**, 133-167 (2009).
4. Krilov, L.R. Adenovirus infections in the immunocompromised host. *Pediatr Infect Dis J* **24**, 555-556 (2005).
5. Hogg, J.C., *et al.* In situ hybridization studies of adenoviral infections of the lung and their relationship to follicular bronchiectasis. *Am Rev Respir Dis* **139**, 1531-1535 (1989).
6. Hayashi, S. & Hogg, J.C. Adenovirus infections and lung disease. *Curr Opin Pharmacol* **7**, 237-243 (2007).
7. Lewis, P.F., *et al.* A community-based outbreak of severe respiratory illness caused by human adenovirus serotype 14. *J Infect Dis* **199**, 1427-1434 (2009).
8. Metzgar, D., *et al.* Abrupt emergence of diverse species B adenoviruses at US military recruit training centers. *J Infect Dis* **196**, 1465-1473 (2007).
9. Zhu, Z., *et al.* Outbreak of acute respiratory disease in China caused by B2 species of adenovirus type 11. *J Clin Microbiol* **47**, 697-703 (2009).
10. Landau, D. Epithelial paracellular proteins in health and disease. *Curr Opin Nephrol Hypertens* **15**, 425-429 (2006).
11. Chavakis, T., Preissner, K.T. & Santoso, S. Leukocyte trans-endothelial migration: JAMs add new pieces to the puzzle. *Thromb Haemost* **89**, 13-17 (2003).
12. Barton, E.S., *et al.* Junction adhesion molecule is a receptor for reovirus. *Cell* **104**, 441-451 (2001).
13. Bergelson, J.M., *et al.* Isolation of a common receptor for Coxsackie B viruses and adenoviruses 2 and 5. *Science* **275**, 1320-1323 (1997).
14. Geraghty, R.J., Krummenacher, C., Cohen, G.H., Eisenberg, R.J. & Spear, P.G. Entry of alphaherpesviruses mediated by poliovirus receptor-related protein 1 and poliovirus receptor. *Science* **280**, 1618-1620 (1998).
15. Wessler, S. & Backert, S. Molecular mechanisms of epithelial-barrier disruption by *Helicobacter pylori*. *Trends Microbiol* **16**, 397-405 (2008).

16. Coyne, C.B. & Bergelson, J.M. Virus-Induced Abl and Fyn Kinase Signals Permit Coxsackievirus Entry through Epithelial Tight Junctions. *Cell* **124**, 119-131 (2006).
17. Kuba, K., *et al.* A crucial role of angiotensin converting enzyme 2 (ACE2) in SARS coronavirus-induced lung injury. *Nat Med* **11**, 875-879 (2005).
18. Sims, A.C., *et al.* Severe acute respiratory syndrome coronavirus infection of human ciliated airway epithelia: role of ciliated cells in viral spread in the conducting airways of the lungs. *J Virol* **79**, 15511-15524 (2005).
19. Mercer, J., Schelhaas, M. & Helenius, A. Virus Entry by Endocytosis. *Annu Rev Biochem* **79**, 803-833 (2010).
20. Pickles, R.J., Fahrner, J.A., Petrella, J.M., Boucher, R.C. & Bergelson, J.M. Retargeting the coxsackievirus and adenovirus receptor to the apical surface of polarized epithelial cells reveals the glycocalyx as a barrier to adenovirus-mediated gene transfer. *J Virol* **74**, 6050-6057 (2000).
21. Walters, R.W., *et al.* Basolateral localization of fiber receptors limits adenovirus infection from the apical surface of airway epithelia. *J Biol Chem* **274**, 10219-10226 (1999).
22. Hicks, W., Jr., *et al.* Isolation and characterization of basal cells from human upper respiratory epithelium. *Exp Cell Res* **237**, 357-363 (1997).
23. Peter, I., *et al.* Immunotherapy for murine K1735 melanoma: combinatorial use of recombinant adenovirus expressing CD40L and other immunomodulators. *Cancer Gene Ther* **9**, 597-605 (2002).
24. Conron, M., *et al.* Alveolar macrophages and T cells from sarcoid, but not normal lung, are permissive to adenovirus infection and allow analysis of NF-kappa b-dependent signaling pathways. *Am J Respir Cell Mol Biol* **25**, 141-149 (2001).
25. Higginbotham, J.N., Seth, P., Blaese, R.M. & Ramsey, W.J. The release of inflammatory cytokines from human peripheral blood mononuclear cells in vitro following exposure to adenovirus variants and capsid. *Hum Gene Ther* **13**, 129-141 (2002).
26. Stillie, R., Farooq, S.M., Gordon, J.R. & Stadnyk, A.W. The functional significance behind expressing two IL-8 receptor types on PMN. *J Leukoc Biol* **86**, 529-543 (2009).
27. Chuntharapai, A. & Kim, K.J. Regulation of the expression of IL-8 receptor A/B by IL-8: possible functions of each receptor. *J Immunol* **155**, 2587-2594 (1995).
28. Feniger-Barish, R., Yron, I., Meshel, T., Matityahu, E. & Ben-Baruch, A. IL-8-induced migratory responses through CXCR1 and CXCR2: association with

- phosphorylation and cellular redistribution of focal adhesion kinase. *Biochemistry* **42**, 2874-2886 (2003).
29. Weyand, N.J., *et al.* Monoclonal antibody detection of CD46 clustering beneath *Neisseria gonorrhoeae* microcolonies. *Infect Immun* **74**, 2428-2435 (2006).
 30. Zaidel-Bar, R., Ballestrem, C., Kam, Z. & Geiger, B. Early molecular events in the assembly of matrix adhesions at the leading edge of migrating cells. *J Cell Sci* **116**, 4605-4613 (2003).
 31. Morgan, M.R., Byron, A., Humphries, M.J. & Bass, M.D. Giving off mixed signals--distinct functions of alpha5beta1 and alphavbeta3 integrins in regulating cell behaviour. *IUBMB Life* **61**, 731-738 (2009).
 32. Kim, L.C., Song, L. & Haura, E.B. Src kinases as therapeutic targets for cancer. *Nat Rev Clin Oncol* **6**, 587-595 (2009).
 33. Devalaraja, R.M., *et al.* Delayed wound healing in CXCR2 knockout mice. *J Invest Dermatol* **115**, 234-244 (2000).
 34. Di Cioccio, V., *et al.* Key role of proline-rich tyrosine kinase 2 in interleukin-8 (CXCL8/IL-8)-mediated human neutrophil chemotaxis. *Immunology* **111**, 407-415 (2004).
 35. Hanke, J.H., *et al.* Discovery of a novel, potent, and Src family-selective tyrosine kinase inhibitor. Study of Lck- and FynT-dependent T cell activation. *J Biol Chem* **271**, 695-701 (1996).
 36. Zaiss, A.K., Machado, H.B. & Herschman, H.R. The influence of innate and pre-existing immunity on adenovirus therapy. *J Cell Biochem* **108**, 778-790 (2009).
 37. Zsengeller, Z., Otake, K., Hossain, S.A., Berclaz, P.Y. & Trapnell, B.C. Internalization of adenovirus by alveolar macrophages initiates early proinflammatory signaling during acute respiratory tract infection. *J. Virol.* **74**, 9655-9667 (2000).
 38. Wu, W., *et al.* Human lung innate immune cytokine response to adenovirus type 7. *J Gen Virol* **91**, 1155-1163 (2010).
 39. Mallia, P. & Johnston, S.L. How viral infections cause exacerbation of airway diseases. *Chest* **130**, 1203-1210 (2006).
 40. Leonard, V.H., *et al.* Measles virus blind to its epithelial cell receptor remains virulent in rhesus monkeys but cannot cross the airway epithelium and is not shed. *J Clin Invest* **118**, 2448-2458 (2008).
 41. Amin, R., Wilmott, R., Schwarz, Y., Trapnell, B. & Stark, J. Replication-deficient adenovirus induces expression of interleukin-8 by airway epithelial cells in vitro. *Hum Gene Ther* **6**, 145-153 (1995).

42. Muruve, D.A., Barnes, M.J., Stillman, I.E. & Libermann, T.A. Adenoviral gene therapy leads to rapid induction of multiple chemokines and acute neutrophil-dependent hepatic injury in vivo. *Hum Gene Ther* **10**, 965-976 (1999).
43. Wilmott, R.W., *et al.* Safety of adenovirus-mediated transfer of the human cystic fibrosis transmembrane conductance regulator cDNA to the lungs of nonhuman primates. *Hum Gene Ther* **7**, 301-318 (1996).
44. Haveman, L.M., *et al.* Different cytokine signatures in children with localized and invasive adenovirus infection after stem cell transplantation. *Pediatr Transplant* **14**, 520-528 (2010).
45. Lesokhin, A.M., Delgado-Lopez, F. & Horwitz, M.S. Inhibition of chemokine expression by adenovirus early region three (E3) genes. *J Virol* **76**, 8236-8243 (2002).
46. Baggiolini, M. & Clark-Lewis, I. Interleukin-8, a chemotactic and inflammatory cytokine. *FEBS Lett* **307**, 97-101 (1992).
47. Kobayashi, Y. The role of chemokines in neutrophil biology. *Front Biosci* **13**, 2400-2407 (2008).
48. Gillitzer, R. & Goebeler, M. Chemokines in cutaneous wound healing. *J Leukoc Biol* **69**, 513-521 (2001).
49. Gabellini, C., *et al.* Functional activity of CXCL8 receptors, CXCR1 and CXCR2, on human malignant melanoma progression. *Eur J Cancer* **45**, 2618-2627 (2009).
50. Stupack, D.G. & Cheresh, D.A. Integrins and angiogenesis. *Curr Top Dev Biol* **64**, 207-238 (2004).
51. Burckhardt, C., *et al.* Drifting motions of CAR and immobile α v-integrins trigger adenovirus fiber shedding at the plasma membrane and promote infection. *under consideration* (2011).
52. Wickham, T.J., Mathias, P., Cheresh, D.A. & Nemerow, G.R. Integrins α v β 3 and α v β 5 promote adenovirus internalization but not virus attachment. *Cell* **73**, 309-319 (1993).
53. Pampori, N., *et al.* Mechanisms and consequences of affinity modulation of integrin α (V) β (3) detected with a novel patch-engineered monovalent ligand. *J Biol Chem* **274**, 21609-21616 (1999).
54. Ballana, E., *et al.* Cell adhesion through α v-containing integrins is required for efficient HIV-1 infection in macrophages. *Blood* **113**, 1278-1286 (2009).
55. Mitra, S.K. & Schlaepfer, D.D. Integrin-regulated FAK-Src signaling in normal and cancer cells. *Curr Opin Cell Biol* **18**, 516-523 (2006).

56. Sai, J., Raman, D., Liu, Y., Wikswo, J. & Richmond, A. Parallel phosphatidylinositol 3-kinase (PI3K)-dependent and Src-dependent pathways lead to CXCL8-mediated Rac2 activation and chemotaxis. *J Biol Chem* **283**, 26538-26547 (2008).
57. Arias-Salgado, E.G., *et al.* Src kinase activation by direct interaction with the integrin beta cytoplasmic domain. *Proc Natl Acad Sci U S A* **100**, 13298-13302 (2003).
58. Huveneers, S., *et al.* Integrin alpha v beta 3 controls activity and oncogenic potential of primed c-Src. *Cancer Res* **67**, 2693-2700 (2007).
59. Brown, M.C., Cary, L.A., Jamieson, J.S., Cooper, J.A. & Turner, C.E. Src and FAK kinases cooperate to phosphorylate paxillin kinase linker, stimulate its focal adhesion localization, and regulate cell spreading and protrusiveness. *Mol Biol Cell* **16**, 4316-4328 (2005).
60. Schaller, M.D. & Parsons, J.T. pp125FAK-dependent tyrosine phosphorylation of paxillin creates a high-affinity binding site for Crk. *Mol Cell Biol* **15**, 2635-2645 (1995).
61. Raman, D., Sai, J., Neel, N.F., Chew, C.S. & Richmond, A. LIM and SH3 protein-1 modulates CXCR2-mediated cell migration. *PLoS ONE* **5**, e10050 (2010).
62. Noutsias, M., *et al.* Human coxsackie-adenovirus receptor is colocalized with integrins alpha(v)beta(3) and alpha(v)beta(5) on the cardiomyocyte sarcolemma and upregulated in dilated cardiomyopathy: implications for cardiotropic viral infections. *Circulation* **104**, 275-280 (2001).
63. Ashbourne Excoffon, K.J., Moninger, T. & Zabner, J. The coxsackie B virus and adenovirus receptor resides in a distinct membrane microdomain. *J Virol* **77**, 2559-2567 (2003).
64. Diaz, F., *et al.* Clathrin adaptor AP1B controls adenovirus infectivity of epithelial cells. *Proc Natl Acad Sci U S A* **106**, 11143-11148 (2009).
65. Zen, K., *et al.* Neutrophil migration across tight junctions is mediated by adhesive interactions between epithelial coxsackie and adenovirus receptor and a junctional adhesion molecule-like protein on neutrophils. *Mol Biol Cell* **16**, 2694-2703 (2005).
66. Witherden, D.A., *et al.* The junctional adhesion molecule JAML is a costimulatory receptor for epithelial gammadelta T cell activation. *Science* **329**, 1205-1210 (2010).

Figure legends

Fig. 1: Macrophages facilitate apical adenovirus infection.

(A) Adenovirus infection of polarized epithelial cells. Polarized or subconfluent 16HBE14o were inoculated (inocul) with Ad5 expressing murine IL-2 (mull-2) for 20 h from the apical (ap) or the basal (bl) side with or without previous treatment with 20 mM EDTA for 2 min. Infection was measured by determining mull-2 levels in the supernatants using ELISA. Data represent mean of triplicates and SEM; statistical relevance (p-value) was determined by Student's t-test.

(B) Ad2/5 receptors CAR and $\alpha\beta 3$ and $\alpha\beta 5$ integrins are expressed on epithelial A549 and 16HBE14o cells, indicated by flow cytometry.

(C) TEM of 16HBE114o monolayer on transwell filter with apically added macrophages. Arrowheads indicate viral particles. The inset enlarges an area of interest. **(D)** Quantification of total viral particles in macrophages (n=5) and epithelial cells (n=17).

(E) Apical infection upon addition of macrophages. Polarized 16HBE14o were infected with Ad5_mull2 from the apical side in presence or absence of macrophages, or from the basal side for 20 or 30 h. Data represent mean of triplicates and SEM.

Fig. 2: Conditioned medium from Ad-inoculated macrophages is sufficient to facilitate apical Ad5 infection.

(A) Scheme for standardized conditioned medium (CM) production and epithelial cell stimulation. Macrophages were incubated with Ad2 at 37°C for 4 h. Supernatant CM was centrifuged at 16 000 x g at 4°C for 15 min. Aliquots were stored at -20°C until use. Polarized epithelial cells were stimulated with CM from the apical side (unless

stated otherwise) at 37°C for 4 h, followed by apical infection with Ad5_muLL-2 for 20 h.

(B) Apical infection upon stimulation with CM. Polarized 16HBE14o were stimulated with CM for 4 h or left untreated, and infected from the apical (ap) or basal (bl) side with Ad5_muLL2 for 20 or 30 h. Levels of muLL-2 in the supernatant were determined by ELISA and relative values obtained by normalization against apical infection for 20 h. Data represent means of triplicates and SEM; p-value was determined by Student's t-test.

(C) Time course of CM stimulation. Polarized 16HBE14o were stimulated with CM for 2-20 h, and infected with Ad5_muLL2 for 20 h. Infection was normalized against time point 0.

(D) Apical stimulation with CM is more efficient than basal stimulation. Polarized 16HBE14o cells were stimulated with CM apically (ap), basally (bl) or both for 4 h and infected with Ad5_muLL-2 for 20 h. Infection was normalized against non-treated control.

(E-F) Impact of CM stimulation on the integrity of polarized 16HBE14o cells. Transepithelial electrical resistance (TEER, panel E) and apparent permeability (perm app) of 10 kDa FITC dextran (50 µg/ml apically, 30 min) (panel F) were determined before (0 h, control) and after (4 h) treatment with CM or 20 mM EDTA (grey and black bars in E). Data represent means of triplicates and SEM.

(G) Enhanced apical binding of adenovirus upon CM stimulation. Polarized 16HBE14o cells were treated with control medium or CM, and atto565-labeled Ad2 was cold bound to the apical side. Samples were stained for the basolateral marker β -catenin and nuclei (Hoechst). Z-projections of confocal stacks with sections spaced by 0.19 µm are shown. Bound virions are indicated by white arrow heads. Scale bar = 10 µm.

(H) Quantification of images shown in G. The mean relative fluorescence of Ad2-atto565 from stacks with a surface area of 246.5 μm^2 was plotted from the apical to the basal sides.

Fig. 3: CXCL-8 is an infection stimulating component of CM.

(A) Recombinant human CXCL-8 boosts apical infection with adenovirus. Polarized 16HBE14o cells were treated with CM, CXCL-8 or IFN- γ at indicated concentrations for 4 h, or left untreated prior to apical infection with Ad5_mull-2 for 20 h. Infection was normalized against non-treated controls. Data represent means of triplicates and SEM; p-value was determined by Student's t-test.

(B) Neutralizing antibody against CXCL-8 significantly diminishes apical infection upon CM stimulation. CM was incubated with neutralizing antibodies against CXCL-8 or IL-10 prior to stimulation of polarized 16HBE14o cells or left untreated. Apical infection with Ad5_mull-2 was for 20 h, and normalization against non-treated controls.

(C) Neutralizing antibodies against CXCL-8 receptors CXCR-1 and CXCR-2 significantly reduce apical infection upon CM stimulation. Polarized 16HBE14o cells were incubated with neutralizing antibodies against CXCR-1, CXCR-2 alone and both together prior to CM stimulation. Cells were infected apically with Ad5_mull-2 and infection was normalized against untreated control.

(D) CXCR-1 and CXCR-2 are rapidly activated upon CM stimulation. Surface expressions of CXCR-1 and CXCR-2 were determined by flow cytometry in control 16HBE14o cells or 16HBE14o cells 10 min after stimulation with CM.

(E) CXCR-1 and CXCR-2 are localized on the apical surface of polarized 16HBE14o cells. Polarized 16HBE14o cells were stained for CXCR-1 or CXCR-2 and ZO-1. Nuclei were stained with Hoechst. Z-projections of confocal stacks are shown. Scale bar = 10 μm .

Fig. 4: CXCL-8 is responsible for CM-induced apical translocation of $\alpha\beta 3$ integrin.

(A) Total surface expression of adenovirus receptors CAR, $\alpha\beta 3$ and $\alpha\beta 5$ integrins determined by flow cytometry in untreated cells (black line) or after CM stimulation of confluent A549 cells for 4 h (black line, grey filled). IgG isotype control is shown in grey line.

(B,C) CM and CXCL-8 relocate $\alpha\beta 3$ integrin to the apical side. Polarized A549 cells were stimulated with CM, CXCL-8 or CM incubated with neutralizing antibody against CXCL-8 prior to stimulation. Cells were stained for $\alpha\beta 3$ integrin and confocal stacks were recorded. Z-projections of the stacks are shown. Scale bar = 15 μm . Quantification of the mean relative fluorescence for each section of the stacks covering an area of 246.5 μm^2 , plotted from the apical (ap) to the basal (bl) sections.

(D) Polarized 16HBE14o cells were stimulated with CM, CXCL-8 or CM incubated with neutralizing antibody against CXCL-8 prior to stimulation. Apical cell surface was biotinylated, and biotinylated proteins were pulled down with neutravidin from cell lysates. Aliquots of biotinylated samples and total cell lysate were probed for $\beta 3$ integrin and CD46 on a Western blot.

(E) Polarized 16HBE14o cells were stimulated with CM for 4 h or left untreated. Neutralizing antibodies against $\alpha\beta 3$ or $\alpha\beta 5$ integrins were added for the last hour. Cells were apically infected with Ad5_muLL-2 for 20 h. Graph shows normalized infection compared to untreated control. Data represent means of triplicates and SEM.

(F) Competition assay with soluble forms of Fc-tagged CAR (CARex-Fc) and $\alpha\beta 3$ integrin ($\alpha\beta 3\text{ex-Fc}$) with soluble CD46 (CD46ex-Fc) as control. Polarized 16HBE14o cells were stimulated with CM for 4 h or left untreated. Soluble virus receptors were added from the apical side and incubated at 4°C for 1 h. Cells were apically infected with Ad5_muLL-2 for 20 h. Graph shows normalized infection

compared to untreated control. Data represent means of triplicates and SEM with P-values relative to data indicated by *.

(G) Competition assay with soluble forms of Ad2 fiber knob and Ad35 fiber knob as control. Assay was performed as described for (F).

Fig. 5: CM-stimulated apical $\alpha\text{v}\beta 3$ integrin localization and Ad5 infection are Src-dependent.

(A) Src and paxillin are phosphorylated upon CM stimulation. Confluent 16HBE14o cells were serum-starved for 24 h and subsequently stimulated for 10 min or 4 h with media containing serum, CM, CXCL-8 or CM incubated with neutralizing antibody against CXCL-8 prior to stimulation. Samples were analyzed by Western blot and probed for paxillin (phospho-Y118), Src (phospho-Y416) or tubulin. Note that there is a significant short term signal of paxillin (phospho-Y118) in control (serum-stimulated) cells.

(B) Phospho-paxillin localizes to the apical side upon CM stimulation. Polarized 16HBE14o cells were stimulated with control medium and CM and stained for paxillin (phospho-Y118), ZO-1 and nuclei (Hoechst). Confocal stacks were recorded and z-projections composed. Scale bar = 10 μm .

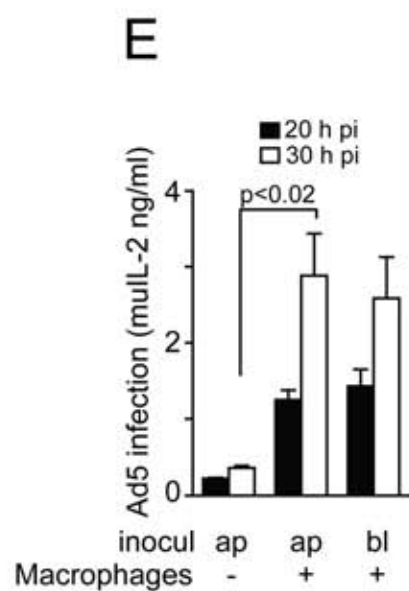
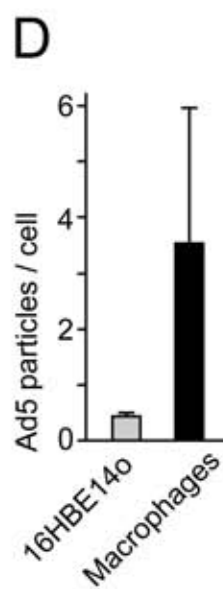
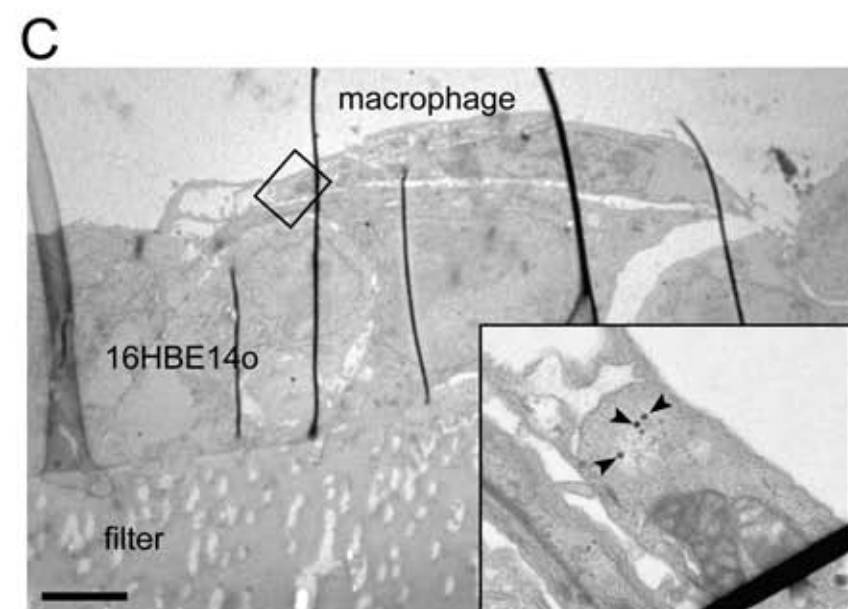
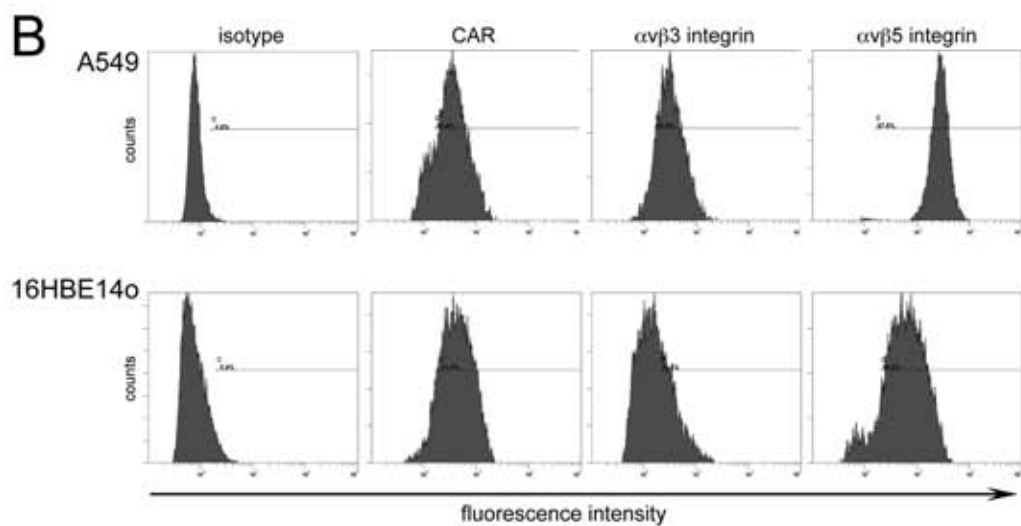
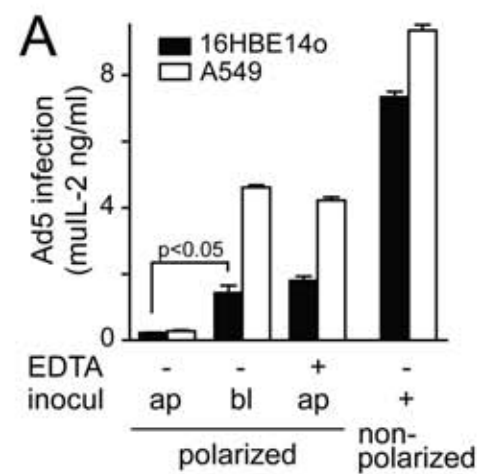
(C) Src-inhibitors PP1 and PP2 inhibit apical Ad5 infection upon CM stimulation. Polarized 16HBE14o cells were treated with DMSO, PP1 and PP2 (10 μM) for 1 h or left untreated (DMSO). Subsequently, cells were stimulated with CM for 4 h, and infected with Ad5_{mulL-2} for 20 h. Infection was normalized against controls. Data represent mean of triplicates and SEM.

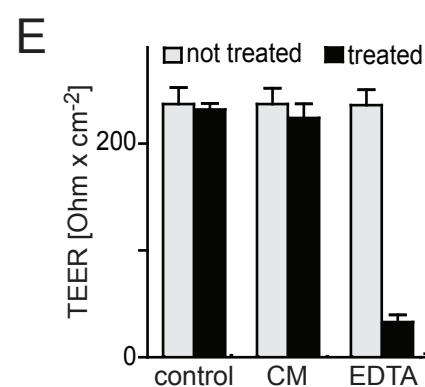
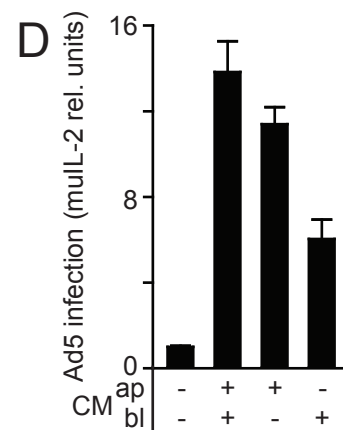
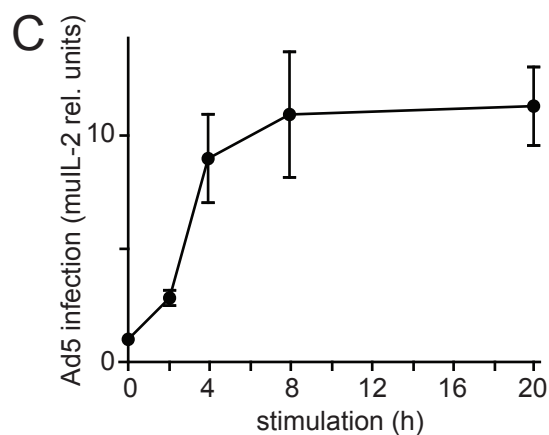
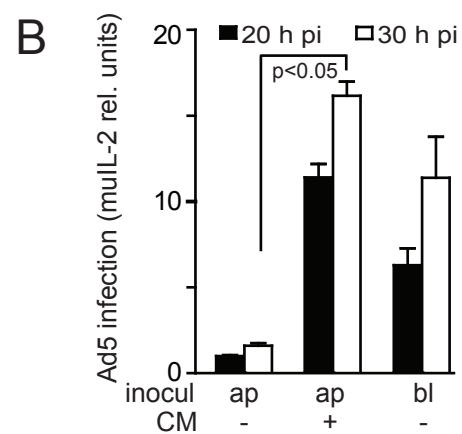
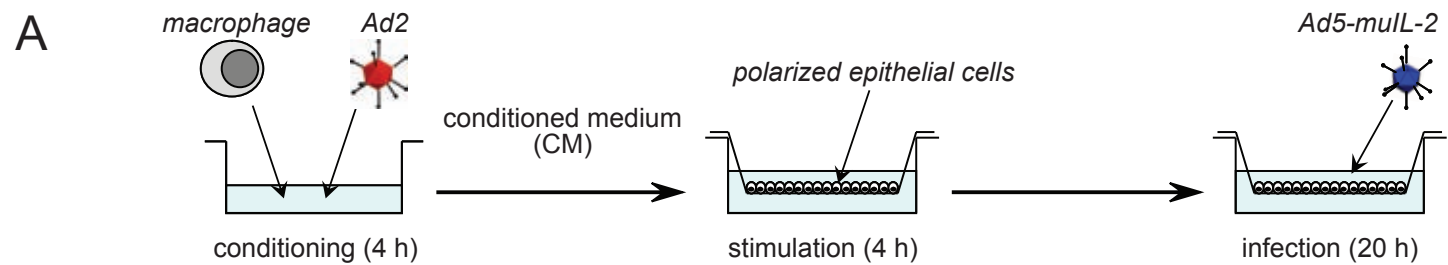
(D) PP1 and PP2 prevent phosphorylation of Src and reduce phosphorylation of paxillin. Confluent 16HBE14o cells were serum starved for 24 h. Cells were treated with PP1 and PP2 (10 μM) for 1 h, and stimulated with CM. Aliquots of total cell lysates were analyzed by Western blot and probed for paxillin (phospho-Y118), Src (phospho-Y416) or tubulin.

(E) Polarized 16HBE14o cells were treated with DMSO, PP1 or PP2 (10 μ M) for 1 h, and subsequently stimulated with CM for 4 h. Cells were biotinylated on the apical side, lysed and biotinylated proteins were pulled down with neutravidin. Aliquots of biotinylated samples and total cell lysate were probed for β 3 integrin and CD46 on a Western blot.

Fig. 6: Schematic model for apical adenovirus infection route.

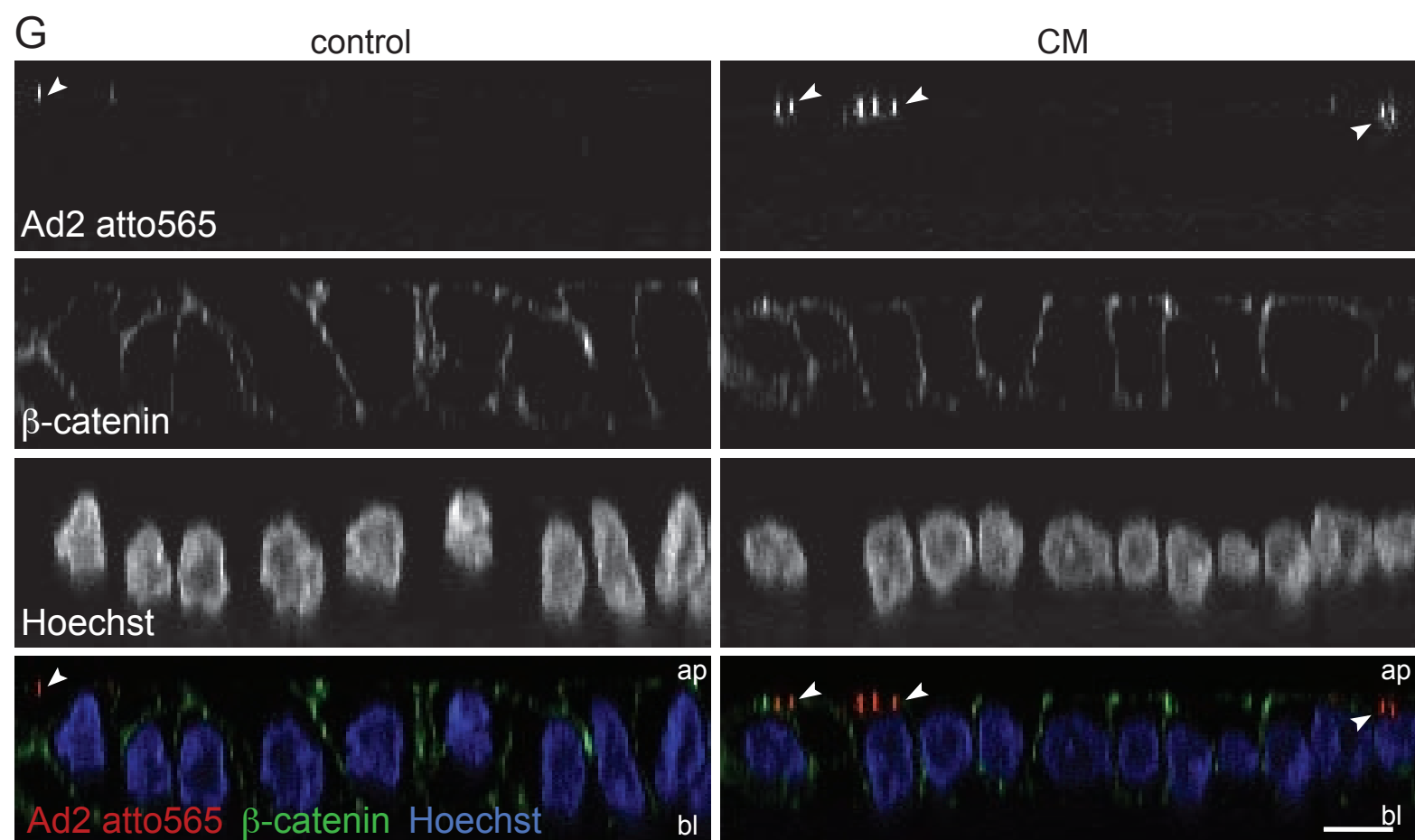
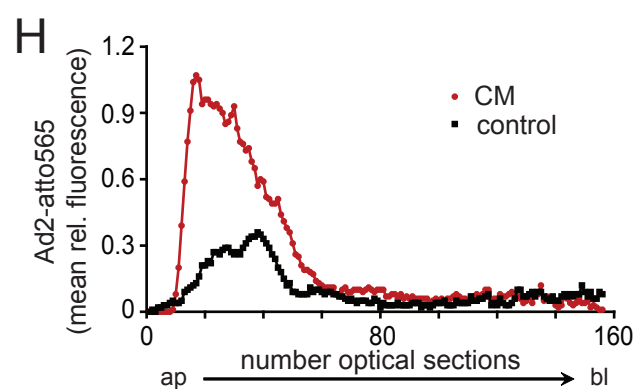
Adenovirus particles are taken up by apical macrophages, which subsequently release cytokines, such as CXCL-8. CXCL-8 triggers a signalling cascade in epithelial cells by activating its receptors CXCR-1 and CXCR-2. In the course of this signalling, c-Src (Src) and paxillin (PXN) are phosphorylated, and this is required for apical localization of phosphorylated paxillin and α v β 3 integrin. Together with apically localized CAR this allows apical binding of adenovirus and infection.

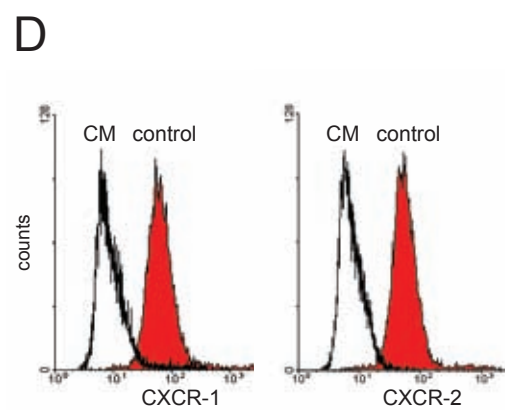
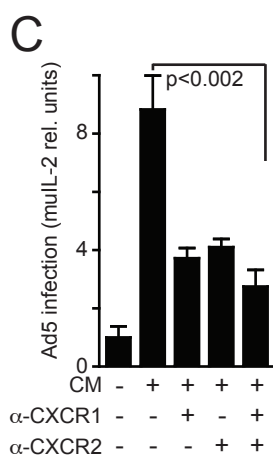
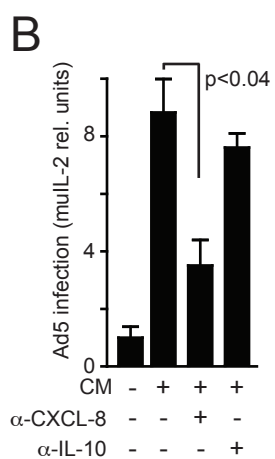
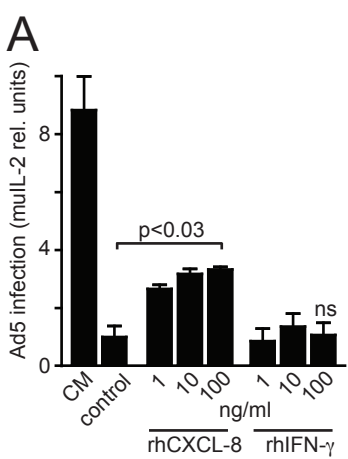




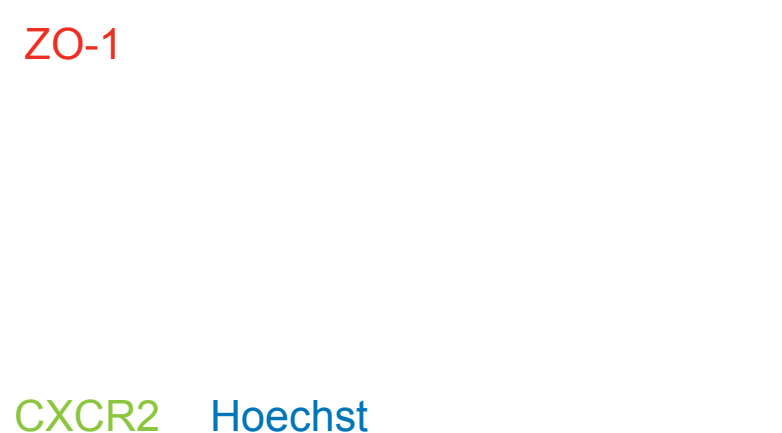
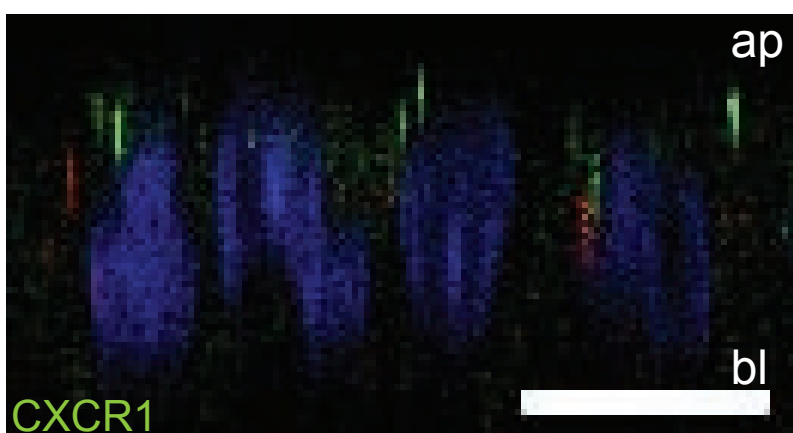
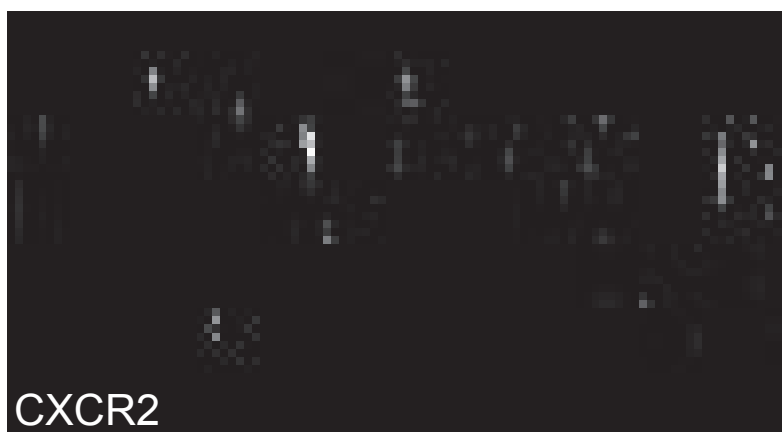
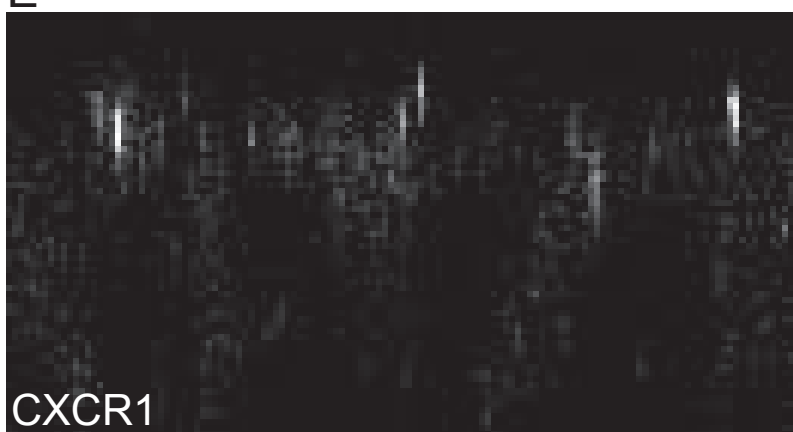
F

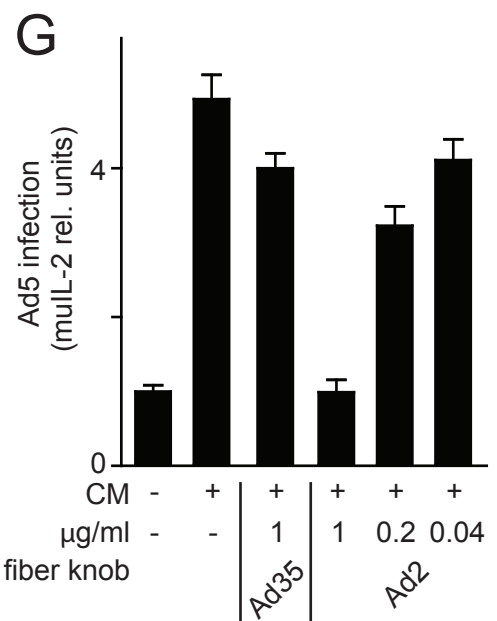
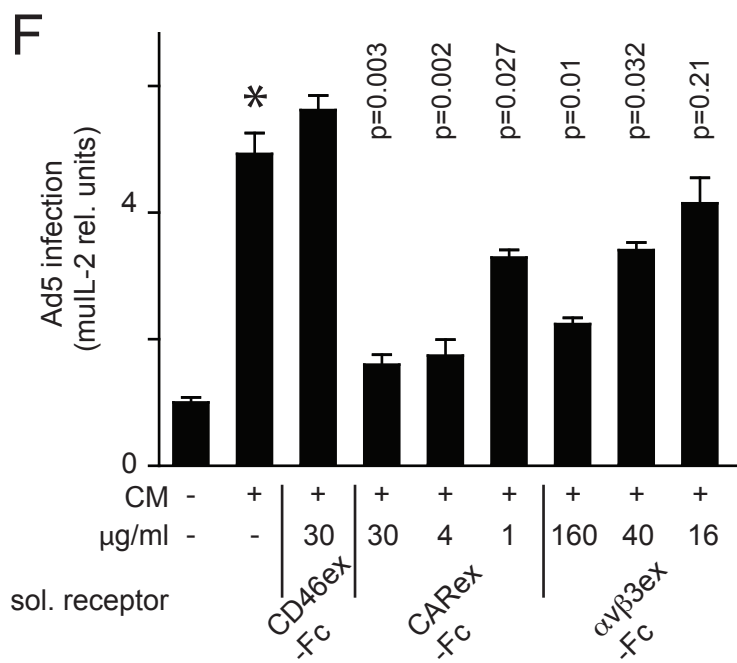
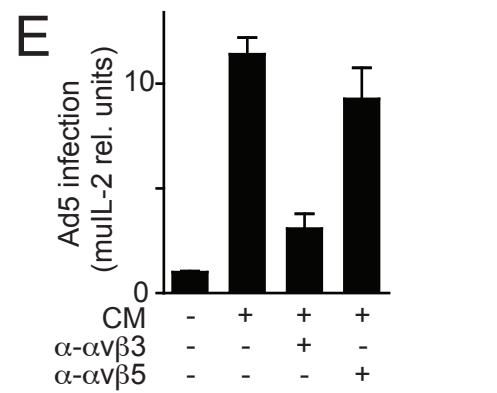
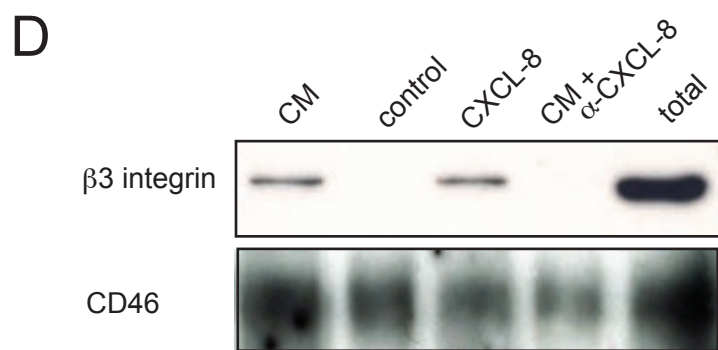
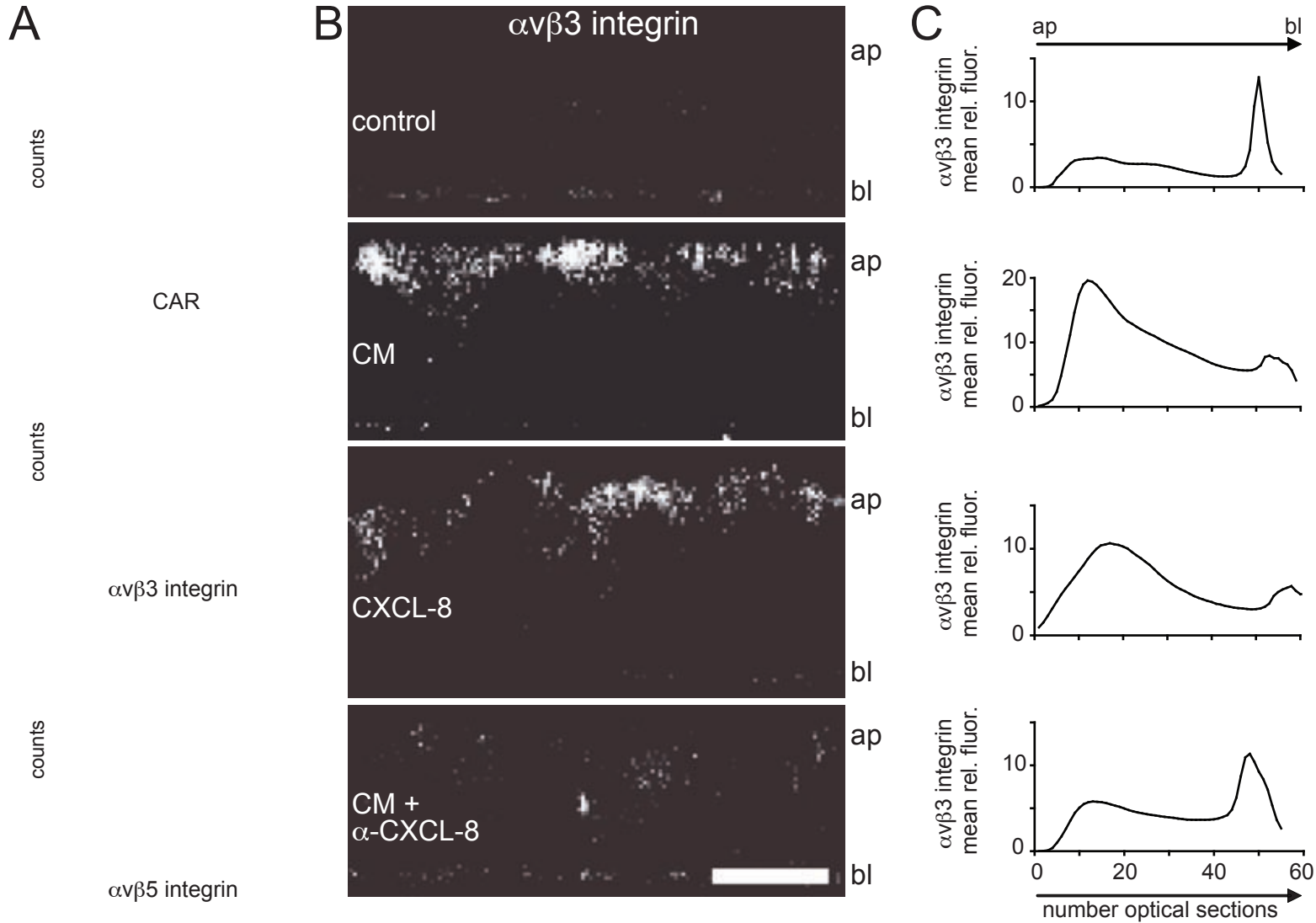
	Perm app x 10 ⁻⁶ (cm ⁻² s ⁻¹)
control	2.506 ± 0.481
CM	0.512 ± 0.004
EDTA	9657 ± 127

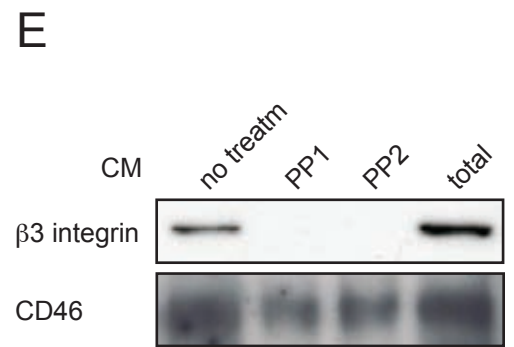
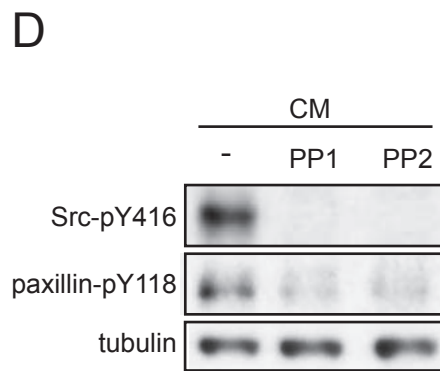
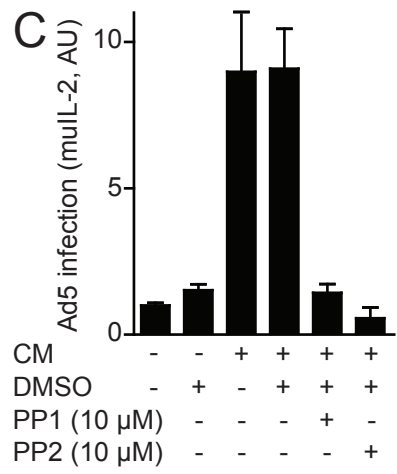
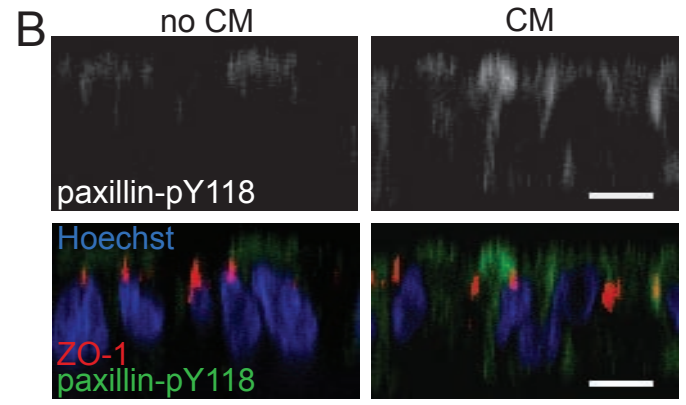
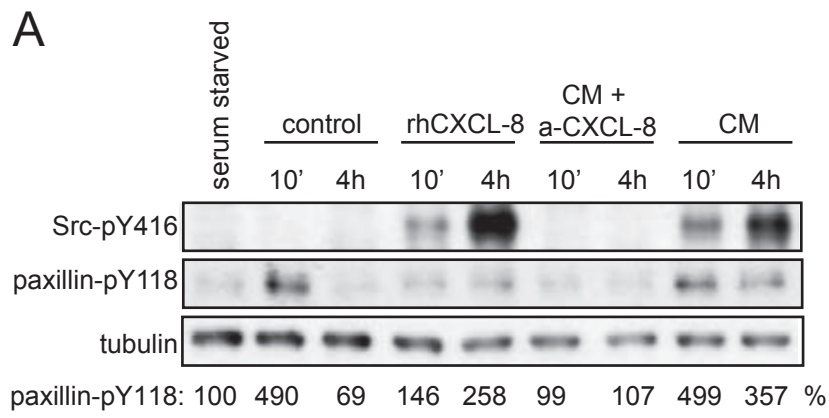


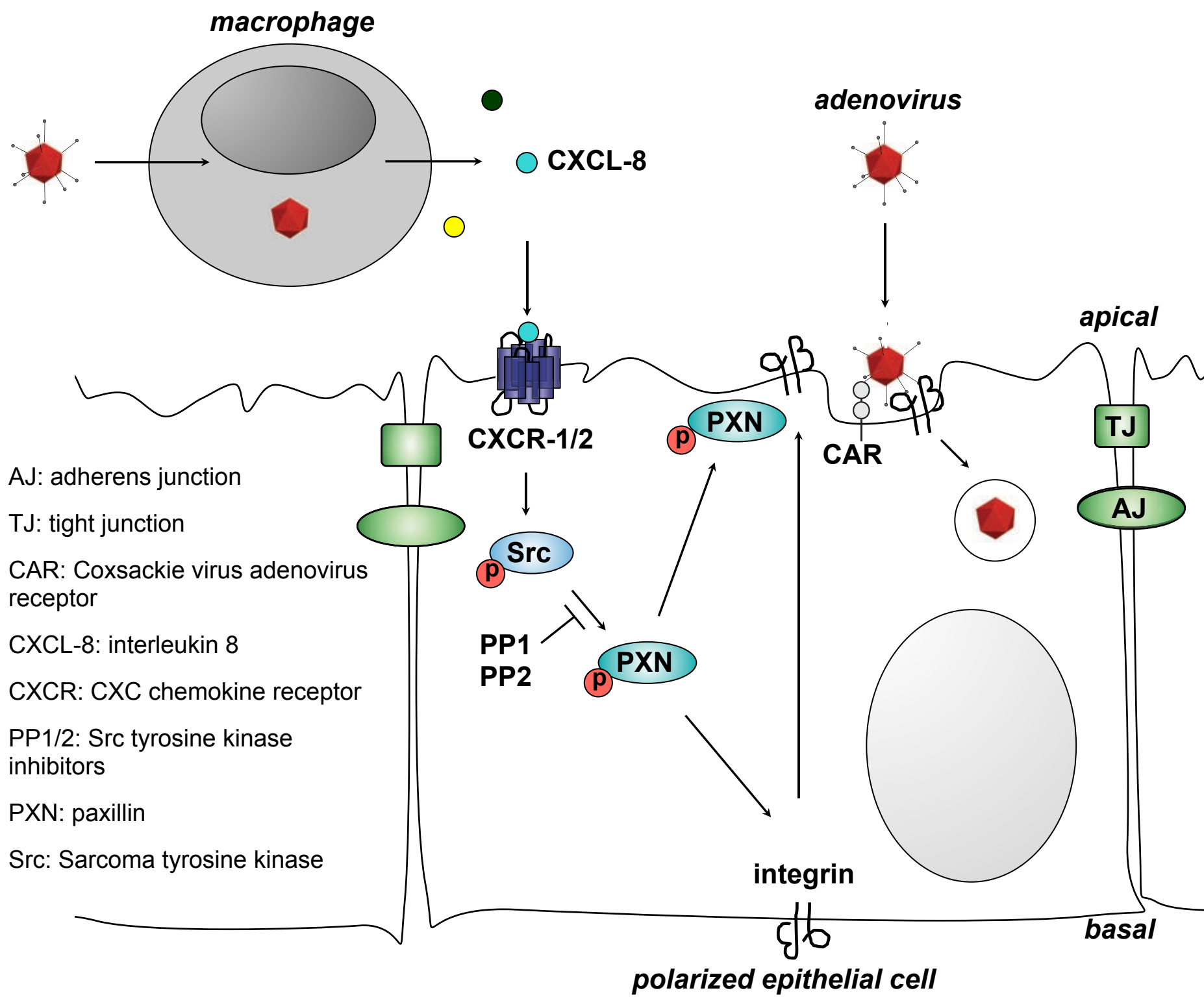


E









Supplemental Information

Materials and Methods

Cell lines, viruses and proteins

Human transformed embryonic retinoblast 911 cells ¹ used for virus propagation were grown in DMEM medium (D6429, Sigma) supplemented with 10% FCS (Invitrogen), 1% L-glutamine and 1% non-essential amino acids (NEA, Sigma). Carcinoma alveolar type II A549 (ATCC) and transformed bronchial epithelial 16HBE14o cells obtained from Dr. D. Gruenert, California Pacific Medical Center Research Institute, San Francisco, USA, ² were grown in RPMI 1640 medium (R8758, Sigma) supplemented with 10% FCS, 1% L-glutamine and 1% NEA. All cells were kept at low passage number at 37°C in a humidified chamber at 5% CO₂. For microscopy of sub-confluent cells, cells were grown to 70% confluency on 18 mm glass cover slips (Menzel Gläser, Braunschweig, Germany). Flow cytometry was performed with cells grown to 100% confluency in 24-well-plate format. Ad5_CMV_eGFP and Ad2 were propagated in 911 cells and isolated and Ad2 was labeled with atto565 (Atto-TEC GmbH, Ad2-atto565) as described previously ³. Ad5_CMV_mull2 was grown as described ⁴. Virus preparations used for stimulation of macrophages were tested for possible endotoxin contaminations with Endochrome Endpoint Assay Kit (Charles River Laboratories). Endotoxin levels were below 0.003 U/ml. Soluble CD46, CAR, $\alpha\beta$ 3 integrin, Ad2 fiber knob or Ad35 fiber knob proteins were used as described ^{5,6}.

Macrophage cell culture

Macrophages were differentiated from human peripheral blood monocytes as described previously ⁷. In brief, peripheral blood monocytes were isolated from buffy coats (blood donation service, Zurich, Switzerland) by density gradient centrifugation on Histopaque (Sigma). PBMCs were washed intensively in phosphate buffered

saline (PBS) and resuspended in RPMI 1640 supplemented with 1% L-glutamine, 1% penicillin/streptomycin and 10% heat-inactivated human serum (blood donation service). Cells were seeded at a density of 10^7 cells per ml and well in a 6-well-plate (Nunc) and allowed to adhere for 4 h. Non-adherent cells were washed away and adherent cells cultured as described above. Macrophages were obtained without any additional supplements. Cells were kept at 37°C in 5% CO₂ humidified atmosphere. Purity of differentiated cells (approx 4×10^5 cells per 6 well dish) was assessed by flow cytometry with CD14 (BD Biosciences) as monocytes/macrophage marker and yielded in >95% positive cells.

Epithelial monolayers and macrophage co-culture

Establishment of epithelial monolayers and co-cultures was modified after Rothen-Rutishauser ⁸. Briefly, epithelial cells were seeded onto cell culture inserts (3 µm pores, 24-well (353492) or 12-well (353292) format, BD Bioscience) and allowed to settle for 2 days. Seeding to filters occurred at 150% plastic dish confluency in order to compensate for reduction in adhesion area during the differentiation process of the epithelial cells at air-liquid interface. Medium was removed, cells were washed with phosphate buffered saline (PBS) and subsequently kept at an air-liquid-interface supplemented with medium only from the basal side (100 µl in 24-wells, 250 µl in 12-wells). A549 cells required 9-10 days to form a monolayer of appropriate integrity, while 16HBE14o could be used after 6-8 days. To obtain co-cultures, macrophages were seeded on top of epithelial cells from the apical side at a ratio of approximately 2:3, settled for 2 h, unattached cells rinsed off, and co-cultures (5-10 epithelial cells per macrophage) maintained at air-liquid-interface for 24 h prior to use.

TEER and diffusion assay

Integrity of epithelial monolayers was assessed by measuring transepithelial electrical resistance (TEER) and the apparent permeability (P_{app}). TEER was measured with

an EVOM Volt-Ohmmeter (World Precision Instruments). To determine the diffusion rate, 50 µg/ml 10kD FITC-dextran (Sigma-Aldrich) was added to the apical side and cells were incubated for 30 min. Aliquots were taken from the apical and basal side and fluorescence was measured using a Safire monochromator-based microplate detection system (Tecan). The apparent permeability (Perm_{app}) was calculated according to the following equation:

$$\text{Perm}_{\text{app}} = (dq/dt) \times 1/(A \times C_o) [\text{cm}^2\text{s}^{-1}]$$

where dq/dt (µg/s) is the rate of transport, C_o is the initial concentration in the apical compartment (µg/ml) and A is the surface area of the filter (cm^2).

Conditioned medium

Differentiated macrophages were incubated with 0.1 µg Ad2 in 1ml per 6-well (80% confluency) at 37°C for indicated times. Conditioned media were removed and centrifuged at 16 000 x g at 4°C for 5 min. Supernatant of non-treated macrophages was used as control. For the ultracentrifugation control samples were centrifuged at 125 000 x g for 1 h. Heat inactivation was performed at 75°C for 15 min. Aliquots of 0.5 to 1 ml were stored at -20°C until use.

Infections

Monolayers or co-cultures in 24-well format were used for infection studies. Cells were treated with control, CM or recombinant human cytokines as indicated. CXCL-8 was obtained from R&D Systems, the IFN- γ preparation had a concentration of about 10^7 U/ml and was used as described⁹. For blocking experiments, CM was incubated with neutralizing antibodies (R&D Systems) 1 h prior to stimulation of monolayers. For drug studies, polarized epithelial cells were incubated with Src-inhibitors PP1 and PP2 (Enzo Life Sciences) for 1 h prior to stimulation. For competition experiments, polarized 16HBE14o cells were stimulated with CM at 37°C for 4 h, and incubated with soluble CD46, CAR, $\alpha\beta 3$ integrin, Ad2 fiber knob or Ad35 fiber knob at 4°C for 1

h. Cells were infected with 10^5 pfu/well of either Ad5_CMV_mull2 or Ad5_CMV_eGFP reporter virus from the apical or basal side. In case of co-culture experiments medium was changed after 8 h and infection continued for another 12 h on air-liquid interface with 100 μ l of medium in the bottom chamber. In all other experiments medium in both chambers was removed after 1 h and infection proceeded for another 19 h on air-liquid interface with 100 μ l of medium in the bottom chamber. Concentration of mull2 in the media was assessed by mull2 ELISA according to the manufacturer's protocol (BD Biosciences). GFP-expression was visualized by confocal microscopy (CSLM, Leica SP5).

Immunofluorescence

Monolayers were cultured on 12-well cell culture inserts as described above and treated with control (PBS), CM, CXCL-8 or CM preincubated with anti-CXCL-8 neutralizing antibodies for 4 h. Cells were fixed with 3% paraformaldehyde (PFA), quenched with 25 mM NH_4Cl and permeabilized with 0.5% Triton X-100. Filters were quartered and incubated with the 1st antibody at 4°C overnight. The following antibodies were used: mouse monoclonal anti-CAR (E1-1) ¹⁰, mouse monoclonal anti-integrin $\alpha\beta$ 3 (clone LM609, Chemicon), mouse monoclonal anti-integrin $\alpha\beta$ 5 (clone P1F6, Chemicon), mouse monoclonal anti-beta-catenin (clone 14, BD Transduction Laboratories), rabbit anti-claudin 1/2 (clone FL-211, Santa Cruz Biotechnology), mouse monoclonal anti-E-cadherin (clone 1.B.54, Santa Cruz Biotechnology), mouse monoclonal anti-occludin (clone 19, BD Transduction Laboratories), mouse monoclonal anti-ZO-1 (clone 1, BD Transduction Laboratories), rabbit anti-ZO-1 (ab59720, Abcam), rabbit anti-paxillin-pY118 (A00379, GenScript). Secondary antibodies (anti-mouse Alexa488, anti-mouse Alexa594, anti-mouse Cy5, anti-rabbit Alexa594; all from Molecular Probes) were incubated at 4°C for 1 h, post-fixed with 3% PFA, and filter pieces mounted on microscopy slides.

Flow cytometry

Cells were detached with accutase (Sigma), blocked with 10 % human serum for 1 h, and incubated with primary antibodies at 4°C on a rotator for 2 h. Secondary antibodies were incubated at 4°C on a rotator for 1 h. Acquisition was performed with a FACScan (Beckman Coulter FC500 Cytometer). A minimum of 10^4 cells were measured for each condition.

Binding assay

Cells were grown on 12-well cell culture inserts as described above. Ad2-atto565 was allowed to bind to the cells at 4°C for 30 min, fixed with 3% PFA, and stained for tight junction marker or receptor proteins as described above.

Biotinylation assay

Confluent monolayers (12-well format) were washed twice with ice-cold HBSS +/- (Gibco) and biotinylated with 0.5 mg/ml biotin (Sulfo-NHS-SS-Biotin, Pierce) from the apical side at 4°C for 30 min, followed by addition of quenching buffer (0.1 M glycine, 0.3% BSA in HBSS +/-), first to the basal side and then to both sides for 5 min on ice, washed three times with ice-cold HBSS +/- and lysed in NP-40 lysis buffer. Biotinylated proteins were precipitated on neutravidin beads (UltraLink Immobilized NeutrAvidin Protein, Pierce), washed intensively and proteins eluted by boiling the samples in SDS-PAGE loading buffer. Samples were analyzed by SDS-PAGE.

SDS-PAGE and Western blotting

Cell lysates were separated on 10% SDS-PAGE, transferred to Hybond-ECL PVDF 0.45 μ m membrane (Amersham Biosciences) and blocked with 5% dried milk in 50 mM Tris/100 mM sodium chloride/0.1% Tween, pH 7.5 (TBST). The following antibodies were used: mouse monoclonal anti-Src-pY416 (clone 9A6, Millipore/Upstate), rabbit anti-paxillin-pY118 (A00379, GenScript), anti-CD46 (clone

H294, Santa Cruz), rabbit anti-tubulin (T13). Antibodies were diluted in TBST/5% BSA (phospho-antibodies) or TBST/2.5% dried milk (all other antibodies). HRP-conjugated secondary antibodies were detected with ECL-Plus reagents (Amersham Biosciences). Filters were stripped with 100 mM β -mercaptoethanol, 2% SDS, and 62.5 mM Tris/HCl, pH 6.7, for 30 min at 50°C, washed extensively with TBST, blocked with 5% dried milk, and re-probed with control or total antibody.

Microscopy

Confocal laser scanning microscopy was conducted with an inverted Leica SP5 microscope (Leica Microsystems) equipped with a 63x objective (oil immersion; NA, 1.4), a diode laser (405-nm excitation), an argon laser (458/476/488/496/514-nm excitation), and a helium laser (561/594/633-nm excitation). Image processing was performed using ImageJ open software (<http://rsbweb.nih.gov/ni-image/>). Samples for transmission electron microscopy were fixed in 1.5% glutaraldehyde-2% formaldehyde in 0.1 M cacodylate buffer (pH 7.4) for 60 min, followed by postfixation in 1% OsO₄ and 1.5% potassium-ferricyanide at RT for 1 h, and staining with 3% uranylacetate over-night. Samples were dehydrated with acetone, embedded in Epon, ultrathin-sectioned and analyzed in a Zeiss EM10.

Supplemental figure legends

Fig. S1: Adenovirus infection of polarized epithelial cells.

(A) Ad5 infection of polarized epithelial cells. Polarized 16HBE14o were infected with Ad5 expressing eGFP from apical side for 20 h, with or without treatment with 20 mM EDTA for 2 min or from the basal side. Infected cells appear green, nuclei are stained with Hoechst (blue) and a β -catenin staining (shown in red) visualizes the cell outlines. Scale bar = 50 μ m.

(B) Quantification of eGFP expression normalized against Hoechst staining, including apical infection (ap) and basolateral infection (bl). Data represent means of triplicates and SEM. Statistical relevance (p-value) was determined by Student's t-test.

Fig. S2: Macrophages are not infected with adenovirus

(A) Ad5 does not infect primary human macrophages, but 16HBE14o cells. PBMC-derived macrophages or subconfluent 16HBE14o cells were infected with Ad5_mull-2 for 20 and 45 h, and expression of mull-2 was measured by ELISA, as described in methods.

(B) Adenovirus receptor CAR is low and $\alpha\beta$ 3/5 integrins are moderately abundant on M Φ s. PBMC-derived macrophages were stained for CAR, $\alpha\beta$ 3 and $\alpha\beta$ 5 integrins and analyzed by flow cytometry.

Fig. S3: Infection stimulating activity of conditioned medium is soluble and heat sensitive.

(A) Conditioned medium (CM) was centrifuged at 125 000 xg for 1 h, and infection normalized against non-treated cells. Data represent means of triplicates and SEM; statistical relevance (p-value) was determined by Student's t-test.

(B) Heat treatment abrogates CM stimulating properties. CM was heat inactivated at 75°C for 15 min, and infection normalized against non-treated cells.

Fig. S4: Cytokine expression from Ad2 inoculated human macrophages.

PBMC-derived macrophages were inoculated with 0.1 µg Ad2 per 6-well (~80% confluency). Conditioned medium (CM) was analyzed for indicated cytokines by BioPlex assay 4 and 8 h post inoculation. The experiment was repeated once with similar results.

Fig. S5: $\alpha\beta 5$ integrin localization is not affected by CM.

(A) Polarized A549 cells were stimulated with CM or left untreated. Cells were stained for $\alpha\beta 5$ integrin and confocal stacks were recorded. Z-projections of stacks are shown. Scale bar = 15 µm.

(B) Quantification of panel A. The mean relative fluorescence for each section of the stacks covering an area of 246.5 µm² was measured and plotted from the apical (ap) to the basal (bl) sections.

(C) Polarized 16HBE14o cells were stimulated with CM or left untreated. Cells were stained for CAR and ZO-1, nuclei were stained with Hoechst. Z-projections of stacks are shown with the white arrowhead indicating dislocated CAR upon stimulation. Scale bar = 10 µm.

Fig. S6: The c-Src inhibitors PP1 or PP2 block the appearance of pY118 paxillin upon stimulation of polarized cells with conditioned medium, but do not affect TEER.

(A) Effect of conditioned medium (CM) stimulation on subconfluent cells. Subconfluent A549 cells were stimulated with CM for 4 h, and stained for paxillin (phospho-Y118), and CAR. Nuclei were stained with Hoechst (blue). Confocal

images are shown. Arrow heads indicate enrichments of p-paxillin in CM stimulated cells. Scale bar = 20 μ m.

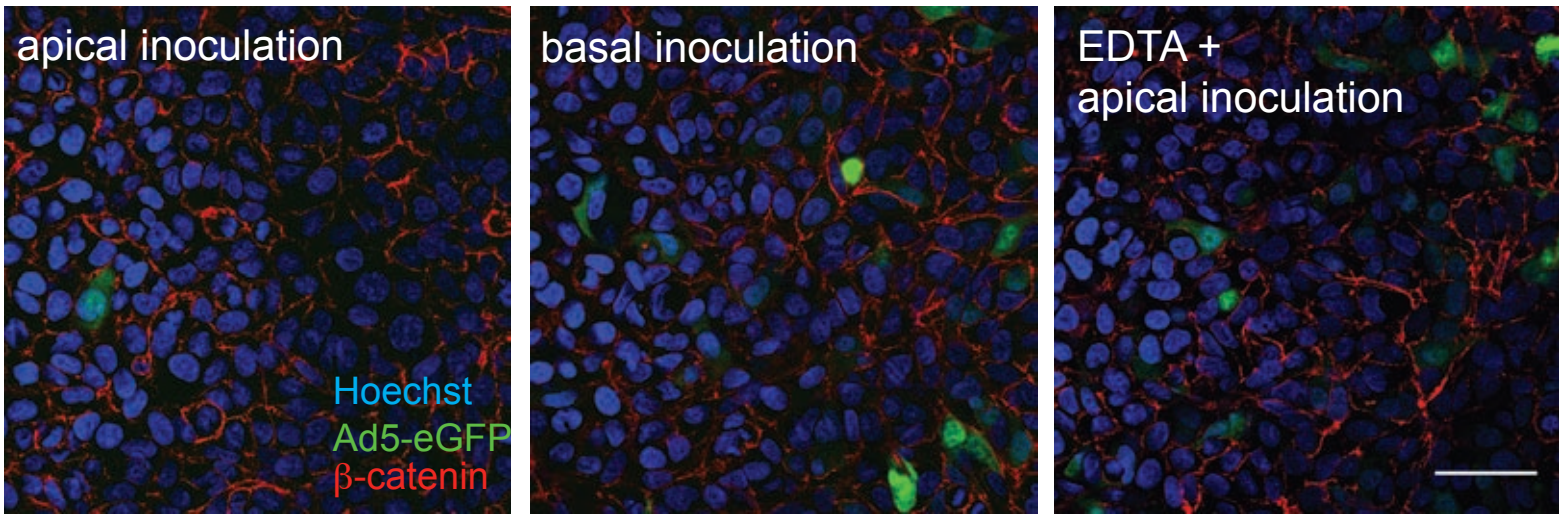
(B) PP1 or PP2 do not affect the transepithelial resistance (TEER) of polarized epithelial cells. Polarized 16HBE14o cells were treated with CM, DMSO, PP1 and PP2 (10 μ M) for 1 h and TEER measured before (0 h) and after (1 h) treatment.

Supplemental references

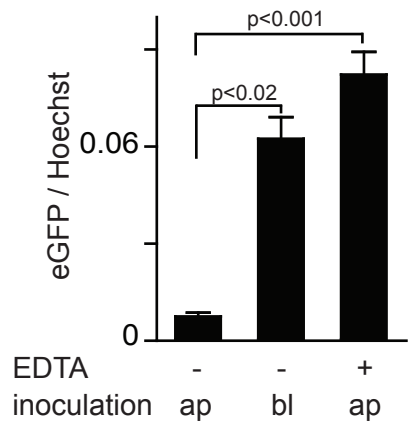
1. Fallaux, F.J., *et al.* Characterization of 911: a new helper cell line for the titration and propagation of early region 1-deleted adenoviral vectors. *Hum Gene Ther* **7**, 215-222 (1996).
2. Gruenert, D.C., Basbaum, C.B. & Widdicombe, J.H. Long-term culture of normal and cystic fibrosis epithelial cells grown under serum-free conditions. *In Vitro Cell Dev Biol* **26**, 411-418 (1990).
3. Suomalainen, M., *et al.* Microtubule-dependent minus and plus end-directed motilities are competing processes for nuclear targeting of adenovirus. *J. Cell Biol.* **144**, 657-672 (1999).
4. Peter, I., *et al.* Immunotherapy for murine K1735 melanoma: combinatorial use of recombinant adenovirus expressing CD40L and other immunomodulators. *Cancer Gene Ther* **9**, 597-605 (2002).
5. Trinh, H., *et al.* Avidity binding of human adenovirus serotypes 3 and 7 to the membrane cofactor CD46 triggers infection. *submitted to J. Virol.* (2011).
6. Burckhardt, C., *et al.* Drifting motions of CAR and immobile α v-integrins trigger adenovirus fiber shedding at the plasma membrane and promote infection. *submitted to Cell Host Microbe* (2011).
7. Miller, M.D., Warmerdam, M.T., Gaston, I., Greene, W.C. & Feinberg, M.B. The human immunodeficiency virus-1 nef gene product: a positive factor for viral infection and replication in primary lymphocytes and macrophages. *J Exp Med* **179**, 101-113 (1994).
8. Rothen-Rutishauser, B.M., Kiama, S.G. & Gehr, P. A three-dimensional cellular model of the human respiratory tract to study the interaction with particles. *Am J Respir Cell Mol Biol* **32**, 281-289 (2005).

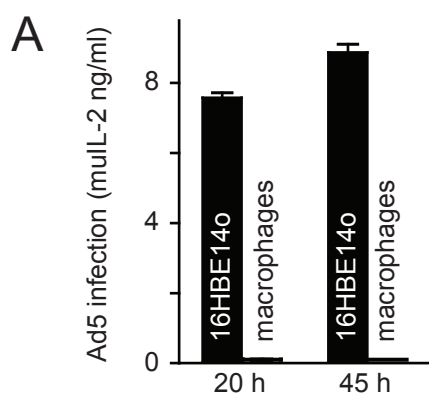
9. Aguet, M., Dembic, Z. & Merlin, G. Molecular cloning and expression of the human interferon-gamma receptor. *Cell* **55**, 273-280 (1988).
10. Ebbinghaus, C., *et al.* Functional and selective targeting of adenovirus to high affinity Fcγ receptor I positive cells using a bispecific hybrid adaptor. *J. Virol.* **75**, 480-489 (2001).

A

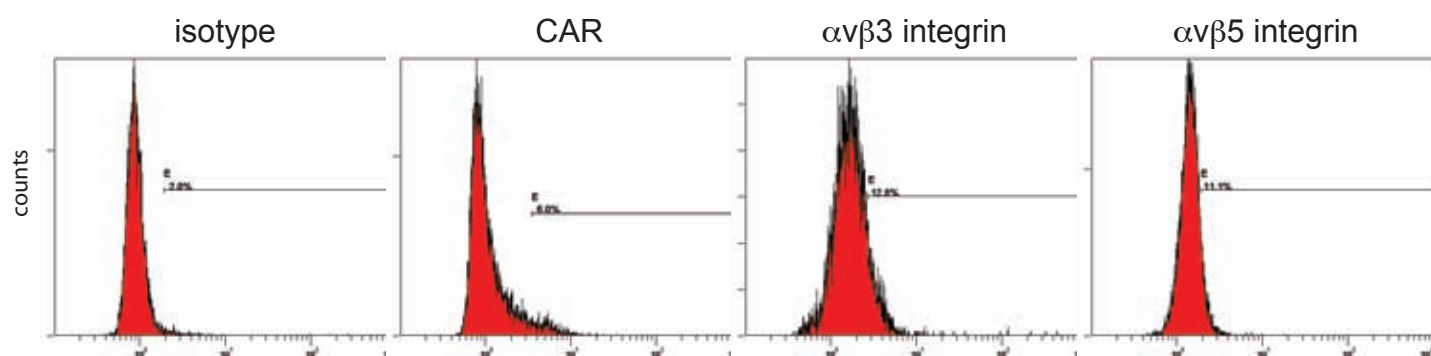


B

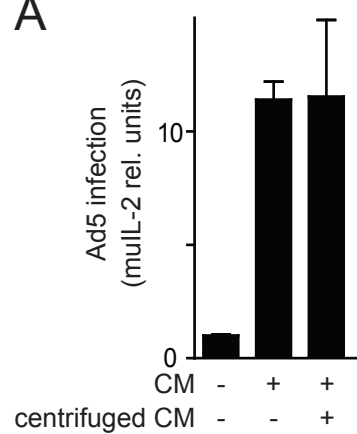




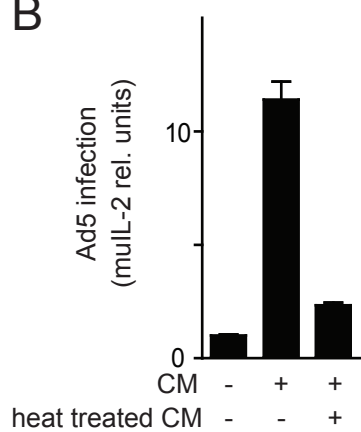
B Macrophages



A



B



cytokine	4 h pi	8 h pi
IL-1 β	-	-
IL-4	-	-
IL-6	+	+
CXCL-8	++	++
IL-10	+	-
IL-12/p70	-	-
IL-13	-	-
IL-15	-	-
IL-17	-	-
IFN- α 2	-	-
IFN- γ	-	+
TNF- α	+	++

